On the Feasibility of Full-Duplex Relaying in Multiple-Antenna Cellular Networks

Konstantinos Ntontin, Marco Di Renzo, Christos Verikoukis

▶ **To cite this version:**

Konstantinos Ntontin, Marco Di Renzo, Christos Verikoukis. On the Feasibility of Full-Duplex Relaying in Multiple-Antenna Cellular Networks. IEEE Transactions on Communications, 2017, 65 (5), pp.2234 - 2249. 10.1109/TCOMM.2017.2668399 . hal-01880007

HAL Id: hal-01880007
https://hal.science/hal-01880007

Submitted on 7 Jul 2020

HAL is a multi-disciplinary open access archive for the deposit and dissemination of scientific research documents, whether they are published or not. The documents may come from teaching and research institutions in France or abroad, or from public or private research centers.

L'archive ouverte pluridisciplinaire **HAL**, est destinée au dépôt et à la diffusion de documents scientifiques de niveau recherche, publiés ou non, émanant des établissements d'enseignement et de recherche français ou étrangers, des laboratoires publics ou privés.

On the Feasibility of Full-Duplex Relaying in Multiple-Antenna Cellular Networks

Konstantinos Ntontin, *Member, IEEE*, Marco Di Renzo, *Senior Member, IEEE*, and Christos Verikoukis, *Senior Member, IEEE*

***Abstract*—In this paper, we perform a system-level feasibility analysis of full-duplex (FD) relay-aided cellular networks that are equipped with multiple antennas at the base stations (BSs) and relay nodes (RNs). The aim is to understand whether FD relaying is capable of enhancing the rate of cellular networks. With the aid of tools from stochastic geometry, we develop a tractable approach for computing the percentile rate, which allows us to gain insights on the impact of FD relaying for both cell-edge and cell-median mobile terminals (MTs) subject to network interference. Contrary to previous works that do not take into account the network interference, the framework reveals that even in the absence of self interference at the FD RNs a network with half-duplex (HD) RNs can outperform its FD counterpart for a moderate number of antennas at the BSs and RNs. On the other hand, the FD-based network can substantially outperform both the HD-based one and the one without RNs for a sufficiently large number of antennas at the BSs and RNs and substantially small self-interference power effect at the RNs. Finally, the aforementioned analytical insights are validated by means of Monte Carlo simulations.**

***Index Terms*—Full-Duplex Relaying, Cell Association, Network Interference, Rate, Multiple Antennas.**

I. Introduction

The deployment of relay nodes (RNs) is considered to be a viable option for improving the coverage and rate of cellular networks, especially at the cell-edge regions [1–12] (and references therein). In addition, it has been included in telecommunication standards, such as the IEEE 802.16j working group [13, 14] and the Third Generation Partnership Project's Long Term Evolution Advanced (3GPP LTE-A) [15, 16]. Most of the existing works on relaying consider half-duplex (HD) RNs due to their simplicity [1–8], [13, 15]. However, HD RNs cannot receive and transmit simultaneously on the same channel, which causes an inefficient use of resources since different time slots or frequency bands are required for the reception and transmission phase. Due to this limitation, during the last years several research works started to consider the implementation of full-duplex (FD) RNs, which are capable of receiving and transmitting simultaneously at the same frequency band [9–12], [14, 16]. This makes such a technology quite attractive due to the potential increase in spectral efficiency compared to HD RNs case. However, the most important challenge that designers of FD systems face is how to mitigate or even eliminate the strong self interference at the FD nodes, which is the result of the simultaneous reception and transmission at the same frequency band. Without counteracting this interference, the performance of FD-based networks in terms of error rate and throughput can be worse compared to their HD counterparts [17, 18]. Some indicative ways to mitigate/eliminate such interference are isolation and signal processing techniques, such as using multiple antennas in the latter case [19–21].

The above works show that relaying can be beneficial regarding coverage and rate improvement with respect to the no-RNs case. They consider, however, scenarios that may not apply in practice, such as that base stations (BSs) and RNs are located at fixed positions and that the other-cell interference is Gaussian distributed. These assumptions do not come in agreement with the expected heterogeneous nature of next generation cellular systems in which the number and the position of these nodes are not known a priori [22]. In addition, the aforementioned literature works study isolated point-to-point systems and, hence, such studies cannot give general insights about the usefulness of RNs in a general cellular system. However, a system-level analysis that considers the whole network and not a point-to-point system is essential since FD RNs are subject to higher interference compared to their HD counterparts. This is due to the fact that more nodes transmit at any time instant than the latter case [23]. Consequently, apart from the self interference, the higher network interference that FD RNs are subject to needs also to be counteracted.

In the literature, there have been several works that study the performance of cellular networks from a system-level perspective, but without considering RNs. In particular, for analytical tractability these works consider the so-called stochastic-geometry abstraction modeling in which nodes, such as BSs and mobile terminals (MTs), are modeled as points of a Poisson-point process (PPP) with a particular intensity [24], [25]. Such an approach has been applied to different scenarios of interest, such as the modeling and analysis of downlink [24], multi-antenna [26, 27], heterogeneous [28–30], uplink

Manuscript received July 13, 2016; revised December 19, 2016 ; accepted February 06, 2017. The work was supported in part by the Generalitat de Catalunya (2014-SGR-1551) together with the CellFive (TEC2014-60130-P) and SMART-NRG (MC-IAPP-612294) projects. The work of M. Di Renzo was supported by the European Commission through the H2020-ETN-5G Wireless Research Project (Grant 641985). The associate editor coordinating the review of this paper and approving it for publication was N. Mehta.

K. Ntontin is with the Green, Adaptive, and Intelligent Networking (GAIN) Group, Department of Informatics and Telecommunications, University of Athens, Greece (e-mail: konstantinos.ntontin.1983@ieee.org).

M. Di Renzo is with the Laboratoire des Signaux et Systèmes, Centre National de la Recherche Scientifique, CentraleSupélec, University Paris Sud, Université Paris-Saclay, 91192 Gif-sur-Yvette, France (e-mail: marco.direnzo@lss.supelec.fr).

C. Verikoukis is with the SMARTECH Department, Telecommunications Technological Centre of Catalonia (CTTC/CERCA), Spain (e-mail: cveri@cttc.es).

[31, 32], millimeter-wave [33–35], and FD cellular networks [36, 37], to give some indicative examples.

Against this background and to the best of the authors' knowledge, [38] is the first work that studies relay-aided cellular networks by considering a stochastic-geometry abstraction modeling, where the BSs, RNs, and MTs are modeled as three independent and homogeneous PPPs. By considering decode-and-forward (DF) [39] and HD-based RNs, the main outcomes of [38] are that coverage and rate highly depend on the path-loss exponents of the one- and two-hop links and that parameter optimization is needed to achieve gains by using RNs in certain scenarios. Specifically, coverage gains with respect to the no-RNs case are observed, whereas no rate increase is feasible due to the HD constraint of the RNs. Apart from not considering FD RNs, [38] considers only single-antenna nodes. Finally, the system model of [38] is extended in [40] by considering multiple-antenna BSs and HD RNs. The outcome of [40] is that even with a substantially large number of antennas the network with HD RNs cannot outperform in terms of rate its counterpart without RNs due to the HD constraint.

Contribution: Motivated by the lack of a system-level analysis regarding the potential of FD RNs in a cellular system, in this work we consider a stochastic geometry-based network of multiple-antenna BSs and FD RNs in the downlink, which can beamform their signal towards their intended receiver. The consideration of multiple antennas at these nodes is initiated by the fact that a high number of antennas is essential towards mitigating/eliminating both the self interference and the higher network interference that the FD nodes are subject to compared to their HD counterparts. This is due to the effect of multi-antenna transmission with a high number of antennas [41]. For the special case of a single receive antenna at the RNs, we derive an analytical expression of the xth percentile rate, which exhibits a good match with respect to Monte Carlo simulations. In addition, it enables the following insights regarding the comparison with a network with HD RNs:

- In the interference-limited region, the coverage probability of the FD network is smaller than the corresponding one of its HD counterpart even in the absence of the self interference at the RNs. However, the xth percentile rate of the former network, which depends on the coverage probability, can be either smaller or larger than the latter one depending on the path-loss exponent values and the available number of antennas. Such an outcome is in contrast to previous works that do not consider the impact of network interference and show that FD RNs outperform the HD ones in terms of rate when there is no self interference or its power effect at the RNs is small [18, 42].
- As the number of antennas at the BSs and RNs increases, the effect of network interference and self interference is mitigated. This means that there is a crossing point regarding the available number of antennas above which the FD network outperforms the HD one in terms of rate.

The above insights are validated by means of Monte Carlo simulations. These simulations also show that: 1) Higher average rates are achieved for the cell-edge and cell-median users of the network with FD RNs compared to its HD counterpart and the baseline network without RNs, provided that: i) The BSs and RNs are equipped with a sufficiently large number of antennas and ii) The self-interference power level at the RNs is adequately small. 2) No-rate gains are achieved by the HD-based network over the one without RNs due to the HD constraint.

Organization: The rest of this paper is organized as follows: In Section II, the system model is presented. Section III introduces the signal model and the xth percentile rate as the performance metric of interest. In Section IV, we derive an analytical expression of the xth percentile rate, whereas in Section V we derive the corresponding analytical expression for the HD case, which is based on the same analysis, and we compare with the FD one. In Section VI, we provide a discussion regarding the applicability and limitations of the derived expressions. The analytical results are validated in Section VII by means of Monte Carlo simulations. Finally, Section VIII concludes this work.

II. System Model

A. Scenario

We consider a downlink relay-aided cellular network, where the BSs, RNs, and MTs are modeled as points of three independent and homogeneous PPPs, which are denoted by Φ_{BS}, Φ_{RN}, and Φ_{MT} with densities λ_{BS}, λ_{RN}, and λ_{MT}, respectively. BSs are equipped with N_{BS} antennas, RNs use N_{RN}^{Rx} for reception, N_{RN}^{Tx} antennas for transmission[1], and operate in FD mode and, finally, MTs are single-antenna nodes. The BSs and RNs have $\delta \geq 1$ frequency bands at their disposal, which serve the MTs. In addition, we assume that the BSs and RNs have perfect instantaneous channel state information (CSI) regarding their intended RNs and MTs[2]. Furthermore, the RNs have perfect CSI of the channel links from their associated BSs and can have perfect, imperfect, or even no knowledge of the self-interference channel coefficients. Moreover, we assume that the BSs pick randomly with probability $1/\delta$ the frequency band to transmit to a particular MT. In addition, the RNs transmit at the same frequency band with the BSs they are paired with. Finally, in this work we do not consider pilot contamination [41] due to space limitations and the fact that it can be totally eliminated by proper signal-processing techniques [43].

Moreover, we denote a particular target MT by MT_0, which can be served via a one or a two-hop transmission. In the former case, the serving BS is denoted by BS_0, whereas in the latter one the RN that serves MT_0 is denoted by RN_0 and the BS that serves RN_0 is denoted by $\mathrm{BS}_{\mathrm{R0}}$. Without loss of generality and based on the Slivnyak theorem [44, vol. 1, Th. 1.4.5], in this work we study the performance metrics of a MT_0 located at the origin of the bi-dimensional plane.

[1]We assume that the RNs have separate receiving and transmitting units in order to make our model more generic by considering cases with $N_{RN}^{Tx} \neq N_{RN}^{Rx}$. However, our analysis also applies to a shared antenna implementation by using a circulator [12].

[2]Such CSI at the BSs and RNs can be obtained from the uplink channels in a time-division duplexing network.

Finally, we note that the analysis is performed for an arbitrary frequency band and the set of interfering BSs and RNs at the frequency band of interest are denoted by $\Phi_{\mathrm{BS}}^{(\mathrm{I})}$ and $\Phi_{\mathrm{RN}}^{(\mathrm{I})}$, respectively. The cell-association criterion regarding whether the communication between a BS and a MT is performed in one or two hops (through the use of a RN) is introduced in Section II-D.

B. FD Relaying Principle

When the communication is assisted by a RN, it takes place in two time slots in which both the BSs and RNs are allowed to transmit. In particular, at time slot n $\mathrm{BS_{R0}}$ conveys to $\mathrm{RN_0}$ the symbol s_n, whereas at the same time slot $\mathrm{RN_0}$ conveys to $\mathrm{MT_0}$ the symbol $s_{n-1}^{'}$. The latter is the detected symbol of s_{n-1} that $\mathrm{BS_{R0}}$ conveyed to $\mathrm{RN_0}$ at time slot $n-1$. Hence, the received version of s_n at $\mathrm{RN_0}$ is subject to self interference due to the transmission of the symbol $s_{n-1}^{'}$ from $\mathrm{RN_0}$. In addition, the received version of $s_{n-1}^{'}$ at $\mathrm{MT_0}$ is subject to interference from $\mathrm{BS_{R0}}$ due to the transmission of s_n.

In the same way, at time slot $n+1$ $\mathrm{BS_{R0}}$ conveys to $\mathrm{RN_0}$ the symbol s_{n+1}, which is subject to self interference due to the transmission from $\mathrm{RN_0}$ at the same slot of the symbol $s_n^{'}$, which is the detected symbol at $\mathrm{RN_0}$ of time slot n. Moreover, the received version of $s_n^{'}$ at $\mathrm{MT_0}$ is subject to interference from $\mathrm{BS_{R0}}$ due to the transmission of s_{n+1}. This way, as $n \to \infty$ the symbol rate of the FD operation asymptotically tends to 1 symbol/slot, which is the same as the direct-communication rate without RNs.

C. Channel Modeling

1) Path-Loss Model: Let r_{X_i,Y_k} be the distance between the nodes X_i and Y_k with path loss $l\left(r_{X_i,Y_k}\right) = \kappa_0 r_{X_i,Y_k}^{\beta_{X,Y}}$, where κ_0 denotes the free-space path loss at a distance of one meter and $\beta_{X,Y} > 2$ denotes the path-loss exponent. Specifically, $\kappa_0 = \left(4\pi/v\right)^2$, where v is the transmission wavelength.

2) Shadowing Model: Besides the distance-dependent path loss, we further assume that the link between the nodes X_i and Y_k is subject to shadow fading, which follows a log-normal distribution [45], whose probability density function (pdf) is

$$f_{S_{X_i,Y_k}}(\xi) = \left[10\log_{10}(e)\Big/\left(\sqrt{2\pi\sigma_{X,Y}^2}\xi\right)\right] \times \exp\left(-\left(10\log_{10}(\xi) - \mu_{X,Y}\right)^2\Big/\left(2\sigma_{X,Y}^2\right)\right), \quad (1)$$

where $\mu_{X,Y}$ and $\sigma_{X,Y}^2$ denote the mean and the variance of the random variable $10\log_{10}\left(S_{X_i,Y_k}\right)$. For mathematical tractability, the expected spatial correlation of shadowing is not considered in this paper.

3) Fast-Fading: Besides path-loss and shadowing, the links between any of the antennas of the X_i and Y_k nodes are subject to a random complex channel gain related to fast fading, which is denoted by h_{X_i,Y_k}. The power gain $\left|h_{X_i,Y_k}\right|^2$ is assumed to follow an exponential distribution (*i.e.*, Rayleigh fading is considered) having mean square value equal to 1. Hence, the pdf of $\left|h_{X_i,Y_k}\right|^2$ is $f_{\left|h_{X_i,Y_k}\right|^2}(\xi) = \exp(-\xi)$.

4) Description of the Self Interference at $\mathrm{RN_0}$*:* The self-interfering signal at $\mathrm{RN_0}$ consists of two parts [12]: i) The direct-path self interference propagating directly from the transmit to the receive chain. It can either comprise the signal propagating directly from the transmit to the receive antennas in a separate antenna structure or the signal reaching the receive chain due to circulator leakage (due to antenna mismatching, for instance) in a shared antenna structure. The power effect of this component can be much larger than the power of the received signal, which can render FD-relaying operations useless [11]. Hence, it is essential that such a component is substantially suppressed so that it is negligible compared to the noise level. This can be realized by the use of highly directional antennas or significant isolation between the transmit and receive antennas of $\mathrm{RN_0}$ and cancellation techniques [12]. In fact, such an important suppression can be achieved without resorting to bulky components and antenna structures [46]. Due to this, in this work we assume that the power effect of the direct path of the self-interfering signal is negligible compared to the noise level. ii) A multipath part due to scattering and reflections from objects in the radio path. We assume that this fast-fading coefficient for each transmit-receive antenna pair of $\mathrm{RN_0}$ is described by a zero-mean complex Gaussian random variable with variance σ_{SI}^2, which depends on the distance-based path loss and the shadowing effects that the scattering components experience before reaching the receive antennas of $\mathrm{RN_0}$. We denote such a matrix by $\mathbf{H}_{\mathrm{SI}} \in \mathbb{CN}^{N_{RN}^{Rx} \times N_{RN}^{Tx}}$. In addition, we assume that $\mathrm{RN_0}$ can have perfect, imperfect, or even no knowledge of the self-interference channel matrix, as we aforementioned in Section II-A[3].

D. Cell Association and Interfering Processes

1) ***Cell Association****:* Let P_T be the total transmit power budget for serving $\mathrm{MT_0}$. Let $P_{\mathrm{BS_0}}$, $P_{\mathrm{RN_0}}$, and $P_{\mathrm{BS_{R0}}}$ denote the transmit powers of $\mathrm{BS_0}$, $\mathrm{RN_0}$, and $\mathrm{BS_{R0}}$, respectively. In order to ensure the total power constraint [39] as our design aim, they are defined by $P_{\mathrm{BS_0}} = P_T$, $P_{\mathrm{RN_0}} = (1-K_T)P_T$, and $P_{\mathrm{BS_{R0}}} = K_T P_T$, where $0 < K_T < 1$ is a power-splitting coefficient.

The triplet $\mathrm{BS_0}$, $\mathrm{RN_0}$, and $\mathrm{BS_{R0}}$ is identified by using the following cell-association criteria:

$$\begin{aligned}
\mathrm{BS_0} &= \underset{\mathrm{BS}_i \in \Phi_{\mathrm{BS}}}{\arg\min} \left\{ \frac{l\left(r_{\mathrm{BS}_i,\mathrm{MT_0}}\right)}{P_T S_{\mathrm{BS}_i,\mathrm{MT_0}}} \right\} \\
\mathrm{RN_0} &= \underset{\mathrm{RN}_k \in \Phi_{\mathrm{RN}}}{\arg\min} \left\{ \frac{l\left(r_{\mathrm{RN}_k,\mathrm{MT_0}}\right)}{(1-K_T)P_T S_{\mathrm{RN}_k,\mathrm{MT_0}}} \right\} \\
\mathrm{BS_{R0}} &= \underset{\mathrm{BS}_i \in \Phi_{\mathrm{BS}}}{\arg\min} \left\{ \frac{l\left(r_{\mathrm{BS}_i,\mathrm{RN_0}}\right)}{K_T P_T S_{\mathrm{BS}_i,\mathrm{RN_0}}} \right\}.
\end{aligned} \quad (2)$$

The association criteria in (2) ensure that $\mathrm{MT_0}$ receives the highest power from the available BSs and RNs in the case that it is associated with a BS and RN, respectively, as well as that the serving RN, $\mathrm{RN_0}$, receives the highest power from the available BSs.

Let the triplet of network elements $\mathrm{BS_0}$, $\mathrm{RN_0}$, and $\mathrm{BS_{R0}}$ from (2). The typical MT, $\mathrm{MT_0}$, is served either via a one-

[3]In the case of perfect CSI, $\mathrm{RN_0}$ can eliminate the self-interference signal with proper precoding vectors as in [19] and, hence, $\sigma_{\mathrm{SI}}^2 = 0$. In the case of imperfect CSI, we assume that the residual interference that remains after the cancellation method follows a distribution with variance σ_{SI}^2.

or a two-hop link according to the cell-association criterion as follows:

$$\begin{cases} \text{One hop}, & \text{if } \frac{l\left(r_{\mathrm{BS}_0,\mathrm{MT}_0}\right)}{\mathcal{B}_{\mathrm{BS}} P_T S_{\mathrm{BS}_0,\mathrm{MT}_0}} \leq \frac{l\left(r_{\mathrm{RN}_0,\mathrm{MT}_0}\right)}{\mathcal{B}_{\mathrm{RN}}(1-K_T) P_T S_{\mathrm{RN}_0,\mathrm{MT}_0}} \\ \text{Two hops}, & \text{otherwise}, \end{cases} \tag{3}$$

where $\mathcal{B}_{\mathrm{BS}}$ and $\mathcal{B}_{\mathrm{RN}}$ are non-negative constants and BS_0, RN_0, $\mathrm{BS}_{\mathrm{R0}}$ are obtained from (2). $\mathcal{B}_{\mathrm{BS}}$ and $\mathcal{B}_{\mathrm{RN}}$ are called bias coefficients and depending on their value they prioritize either the single-hop or the two-hop transmission conditioned on the values of the path-loss exponents. Without loss of generality, we assume that $\mathcal{B}_{\mathrm{RN}} = 1$ and $\mathcal{B}_{\mathrm{BS}} \geq 0$. In particular, the communication takes place in one hop if $\mathcal{B}_{\mathrm{BS}} = \infty$ and in two hops if $\mathcal{B}_{\mathrm{BS}} = 0$.

*2) **Interfering Processes**:* As far as $\Phi_{\mathrm{BS}}^{(\mathrm{I})}$ is concerned, it can be split into two disjoint sets, $\Phi_{\mathrm{BS}}^{(\mathrm{I,1hop})}$ and $\Phi_{\mathrm{BS}}^{(\mathrm{I,2hop})}$, corresponding to the interfering BSs serving their associated MTs either via a one- and two-hop link, respectively. Since the cell association in (2), (3) is distance-dependent, the sets $\Phi_{\mathrm{BS}}^{(\mathrm{I,1hop})}$ and $\Phi_{\mathrm{BS}}^{(\mathrm{I,2hop})}$ are not homogeneous PPPs. For mathematical tractability though, we assume that these sets are homogeneous PPPs with densities $\lambda_{\mathrm{BS}}^{(\mathrm{I,1hop})} = \chi_{1\mathrm{hop}} \lambda_{\mathrm{BS}}^{(\mathrm{I})}$ and $\lambda_{\mathrm{BS}}^{(\mathrm{I,2hop})} = \chi_{2\mathrm{hop}} \lambda_{\mathrm{BS}}^{(\mathrm{I})}$, respectively, where $\chi_{1\mathrm{hop}}$ and $\chi_{2\mathrm{hop}}$ are the probabilities that MT_0 is served via a one- and a two-hop link, respectively. Hence, $\chi_{1\mathrm{hop}} + \chi_{2\mathrm{hop}} = 1$. The process for deriving $\chi_{1\mathrm{hop}}$ and $\chi_{2\mathrm{hop}}$ is introduced in Section IV-A.

In addition, it holds that the number of the interfering RNs is equal to the number of the interfering BSs participating in the two-hop transmissions due to the fact that paired BSs and RNs transmit at the same frequency band. As with $\Phi_{\mathrm{BS}}^{(\mathrm{I,1hop})}$ and $\Phi_{\mathrm{BS}}^{(\mathrm{I,2hop})}$, the set of interfering RNs, which we denote by $\Phi_{\mathrm{RN}}^{(\mathrm{I})}$, is not a homogeneous PPP. However, for mathematical tractability we assume that it is homogeneous with density $\lambda_{\mathrm{RN}}^{(\mathrm{I})} = \chi_{2\mathrm{hop}} \lambda_{\mathrm{BS}}^{(\mathrm{I})}$. The cell association and interfering nodes in the single- and two-hop cases are depicted in Fig. 1.

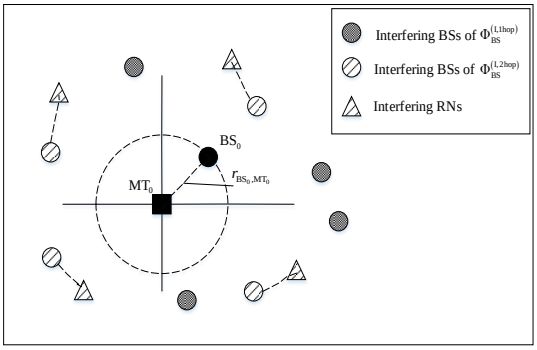

(a) Single-hop communication.

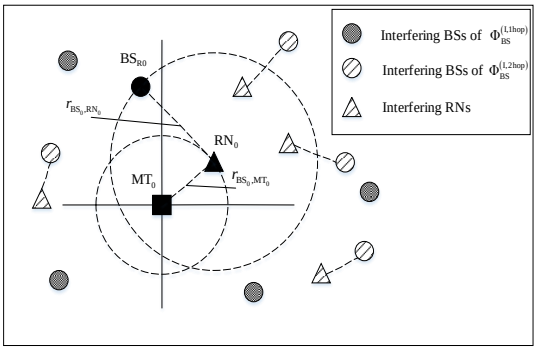

(b) Two-hop communication.

Fig. 1: Cell association and interfering nodes in the single- and two-hop cases.

E. Frequency Band Allocation

We consider that each MT is served by one frequency band, which is chosen randomly with probability $1/\delta$. By assuming that $\lambda_{\mathrm{MT}} = k_{\mathrm{MT}} \lambda_{\mathrm{BS}}$, it holds that the set of the interfering BSs, which we denote by $\Phi_{\mathrm{BS}}^{(\mathrm{I})}$, is a homogeneous PPP of density equal to $\lambda_{\mathrm{BS}}^{(\mathrm{I})} = (k_{\mathrm{MT}}/\delta)\, \lambda_{\mathrm{BS}}$ if $k_{\mathrm{MT}} \ll \delta$, due to the thinning property of a PPP [44] and equal to λ_{BS} if $k_{\mathrm{MT}} \gg \delta$. The latter case holds under the assumption that if δ is smaller than the number of MTs in a cell, only δ MTs are scheduled for downlink transmission and the rest are scheduled at a future period. In such a case, there are different scheduling algorithms to select the MTs to be scheduled, which is out of the scope of this work. In this work, we assume that the MTs are scheduled randomly. The analysis in this work is also valid for general load conditions, such as the case when k_{MT} and δ are comparable. However, the cell-size distribution needs to be known in order to derive the density of the interfering BSs [38], which can be empirically derived from simulations [47].

Notation: The following notation is used throughout this paper: i) s_{k_n} is the transmitted data symbol at time slot n of node k. ii) $\mathcal{Z}_{X,Y} = l\left(r_{X,Y}\right)/S_{X,Y}$ for $X \in \{\mathrm{BS}, \mathrm{RN}\}$ and $Y \in \{\mathrm{RN}, \mathrm{MT}\}$ denotes the ratio of path-loss and shadowing for a generic (X, Y) link. iii) $\sigma_N^2 = 10^{\sigma_N^2(\mathrm{dBm})/10}$ denotes the thermal noise power, where $\sigma_N^2\,(\mathrm{dBm}) = -174 + 10\log_{10}(\mathrm{B_W}) + \mathcal{F}_{\mathrm{dB}}$, $\mathcal{F}_{\mathrm{dB}}$ is the noise figure in dB, and $\mathrm{B_W}$ is the transmission bandwidth of each frequency band. iv) $\eta_{\mathrm{cell}} = (\mathcal{B}_{\mathrm{BS}} P_T)/(\mathcal{B}_{\mathrm{RN}}\,(1 - K_T)\, P_T)$ is a shorthand used for simplifying the writing of (3). v) Recurrent parameters and symbols are included in Table I.

TABLE I: RECURRENT PARAMETERS AND SYMBOLS

Symbol	Meaning
Φ_{X}	PPP of network elements $\mathrm{X} = \{\mathrm{BS}, \mathrm{RN}, \mathrm{MT}\}$
$\Phi_{\mathrm{X}}^{(\mathrm{I})}$	PPP of interfering network elements $\mathrm{X} = \{\mathrm{BS}, \mathrm{RN}\}$
λ_{X}	density of network elements $\mathrm{X} = \{\mathrm{BS}, \mathrm{RN}, \mathrm{MT}\}$
δ	number of frequency bands
BS_0, $\mathrm{BS}_{\mathrm{R0}}$	One- and two-hop serving BSs, respectively
RN_0	serving RN of two-hop transmission
MT_0	reference MT
$\beta_{\mathrm{X,Y}}$	path-loss exponent of the X-to-Y link
$S_{\mathrm{X,Y}}$	shadowing of the X-to-Y link
$h_{\mathrm{X,Y}}$	fast-fading coefficient of the X-to-Y link
P_T	total transmit power
P_{X}	transmit power of network element X
K_T	power-splitting ratio
$\mathcal{B}_{\mathrm{BS}}$, $\mathcal{B}_{\mathrm{RN}}$	bias coefficients
$\chi_{1\mathrm{hop}}$, $\chi_{2\mathrm{hop}}$	one- and two-hop transmission probabilities
σ_N^2	thermal noise power
B_{W}	transmission bandwidth per frequency band
η_{cell}	a shorthand

III. Signal Model and Examined Metric

In this section, expressions of the instantaneous signal-to-interference-plus-noise ratio (SINR) are derived and the performance metric under consideration is presented, which depends on the SINR statistics.

A. Signal Model

1) Single-Hop Transmission: In the case of a single-hop transmission between MT_0 and the selected BS, BS_0, the received signal at MT_0, which is denoted by $y^{(1)}_{\mathrm{MT}_0}$, is given by

$$y^{(1)}_{\mathrm{MT}_0} = \sqrt{(P_T/N_{BS})\,\mathcal{Z}^{-1}_{\mathrm{BS}_0,\mathrm{MT}_0}}\mathbf{h}_{\mathrm{BS}_0,\mathrm{MT}_0}\mathbf{w}_{\mathrm{BS}_0,\mathrm{MT}_0}s_{0_n} + i^{(1)}_{\mathrm{BS},\mathrm{MT}_0} + i^{(2)}_{\mathrm{BS},\mathrm{MT}_0} + i^{(1)}_{\mathrm{RN},\mathrm{MT}_0} + n^{(1)}_{\mathrm{MT}_0}, \quad (4)$$

where $\mathbf{h}_{\mathrm{BS}_0,\mathrm{MT}_0} \in \mathbb{CN}^{1\times N_{BS}}$, $\mathbf{w}_{\mathrm{BS}_0,\mathrm{MT}_0} \in \mathbb{C}^{N_{BS}\times 1}$ is the employed beamforming vector at BS_0, and $E\left\{n^{(1)}_{\mathrm{MT}_0}n^{(1)*}_{\mathrm{MT}_0}\right\} = \sigma^2_N$. In addition, $i^{(1)}_{\mathrm{BS},\mathrm{MT}_0}$, $i^{(2)}_{\mathrm{BS},\mathrm{MT}_0}$ are the interference processes affecting MT_0, which result from the set of BSs constituting the single- and two-hop transmissions, respectively. They are given by

$$i^{(1)}_{\mathrm{BS},\mathrm{MT}_0} = \sum_{\mathrm{BS_i}\in\Phi^{(\mathrm{I,1hop})}_{\mathrm{BS}}} \sqrt{(P_T/N_{BS})\,\mathcal{Z}^{-1}_{\mathrm{BS_i},\mathrm{MT}_0}}\mathbf{h}_{\mathrm{BS_i},\mathrm{MT}_0}\mathbf{w}_{\mathrm{BS_i},\mathrm{MT_i}} \times s_{i_n}\mathbf{1}\left(\mathcal{Z}_{\mathrm{BS_i},\mathrm{MT}_0} > \mathcal{Z}_{\mathrm{BS}_0,\mathrm{MT}_0}\right)$$

$$i^{(2)}_{\mathrm{BS},\mathrm{MT}_0} = \sum_{\mathrm{BS_j}\in\Phi^{(\mathrm{I,2hop})}_{\mathrm{BS}}} \sqrt{K_T(P_T/N_{BS})\,\mathcal{Z}^{-1}_{\mathrm{BS_j},\mathrm{MT}_0}}\mathbf{h}_{\mathrm{BS_j},\mathrm{MT}_0}\mathbf{w}^{Tx}_{\mathrm{BS_j},\mathrm{RN_j}} \times s_{j_n}\mathbf{1}\left(\mathcal{Z}_{\mathrm{BS_j},\mathrm{MT}_0} > \mathcal{Z}_{\mathrm{BS}_0,\mathrm{MT}_0}\right),$$

where $\mathbf{w}_{\mathrm{BS_i},\mathrm{MT_i}}$, $\mathbf{w}^{Tx}_{\mathrm{BS_j},\mathrm{RN_j}}$ are the beamforming vectors related to $\mathrm{BS_i}$ and $\mathrm{BS_j}$, respectively. The indicator functions in (5), $\mathbf{1}\left(\mathcal{Z}_{\mathrm{BS}_i,\mathrm{MT}_0} > \mathcal{Z}_{\mathrm{BS}_0,\mathrm{MT}_0}\right)$ and $\mathbf{1}\left(\mathcal{Z}_{\mathrm{BS}_j,\mathrm{MT}_0} > \mathcal{Z}_{\mathrm{BS}_0,\mathrm{MT}_0}\right)$ for $\mathrm{BS}_i \in \Phi^{(\mathrm{I,1hop})}_{\mathrm{BS}}$ and $\mathrm{BS}_j \in \Phi^{(\mathrm{I,2hop})}_{\mathrm{BS}}$, respectively, originate from the association criterion in (2). $i^{(1)}_{\mathrm{RN},\mathrm{MT}_0}$ is the interference process originating from the interfering RNs towards MT_0, which is given by

$$i^{(1)}_{\mathrm{RN},\mathrm{MT}_0} = \sum_{\substack{\mathrm{RN}_k\in\Phi^{(\mathrm{I})}_{\mathrm{RN}} \\ \mathrm{card}\left\{\Phi^{(\mathrm{I})}_{\mathrm{RN}}\right\}=\mathrm{card}\left\{\Phi^{(\mathrm{I,2hop})}_{\mathrm{BS}}\right\}}} \sqrt{(1-K_T)\,(P_T/N_{RS})\,\mathcal{Z}^{-1}_{\mathrm{RN_k},\mathrm{MT}_0}}\mathbf{h}_{\mathrm{RN_k},\mathrm{MT}_0} \times \mathbf{w}_{\mathrm{RN_k},\mathrm{MT_k}}s'_{k_{n-1}}\mathbf{1}\left(\eta_{\mathrm{cell}}\mathcal{Z}_{\mathrm{RN}_k,\mathrm{MT}_0} > \mathcal{Z}_{\mathrm{BS}_0,\mathrm{MT}_0}\right),$$

where the indicator function in (5) originates from (3).

Since the serving BSs have perfect CSI of the corresponding channel links towards their served MTs or RNs, we assume that the employed beamforming vectors are designed so that they maximize the received signal-to-noise Ratio (SNR). Hence, maximum ratio transmission (MRT) [48] is employed, which means that $\mathbf{w}_{\mathrm{BS}_0,\mathrm{MT}_0} = \frac{\mathbf{h}^H_{\mathrm{BS}_0,\mathrm{MT}_0}}{\left\|\mathbf{h}_{\mathrm{BS}_0,\mathrm{MT}_0}\right\|}$. Consequently, the resulting from (4) SINR at MT_0, which is denoted by $\mathrm{SINR}_{\mathrm{BS}_0,\mathrm{MT}_0}$, is given by

$$\mathrm{SINR}_{\mathrm{BS}_0,\mathrm{MT}_0} = \frac{(P_T/N_{BS})\left\|\mathbf{h}_{\mathrm{BS}_0,\mathrm{MT}_0}\right\|^2\mathcal{Z}^{-1}_{\mathrm{BS}_0,\mathrm{MT}_0}}{\sigma^2_N + I^{(1)}_{\mathrm{BS},\mathrm{MT}_0} + I^{(2)}_{\mathrm{BS},\mathrm{MT}_0} + I^{(1)}_{\mathrm{RN},\mathrm{MT}_0}}, \quad (5)$$

where

$$I^{(1)}_{\mathrm{BS},\mathrm{MT}_0} = \sum_{\mathrm{BS_i}\in\Phi^{(\mathrm{I,1hop})}_{\mathrm{BS}}} (P_T/N_{BS})\,\mathcal{Z}^{-1}_{\mathrm{BS_i},\mathrm{MT}_0}\left|\mathbf{h}_{\mathrm{BS_i},\mathrm{MT}_0}\mathbf{w}_{\mathrm{BS_i},\mathrm{MT_i}}\right|^2 \mathbf{1}\left(\mathcal{Z}_{\mathrm{BS_i},\mathrm{MT}_0} > \mathcal{Z}_{\mathrm{BS}_0,\mathrm{MT}_0}\right)$$

$$I^{(2)}_{\mathrm{BS},\mathrm{MT}_0} = \sum_{\mathrm{BS_j}\in\Phi^{(\mathrm{I,2hop})}_{\mathrm{BS}}} K_T(P_T/N_{BS})\,\mathcal{Z}^{-1}_{\mathrm{BS_j},\mathrm{MT}_0}\left|\mathbf{h}_{\mathrm{BS_j},\mathrm{MT}_0}\mathbf{w}^{Tx}_{\mathrm{BS_j},\mathrm{RN_j}}\right|^2 \mathbf{1}\left(\mathcal{Z}_{\mathrm{BS_j},\mathrm{MT}_0} > \mathcal{Z}_{\mathrm{BS}_0,\mathrm{MT}_0}\right)$$

and

$$I^{(1)}_{\mathrm{RN},\mathrm{MT}_0} = \sum_{\substack{\mathrm{RN}_k\in\Phi^{(\mathrm{I})}_{\mathrm{RN}} \\ \mathrm{card}\left\{\Phi^{(\mathrm{I})}_{\mathrm{RN}}\right\}=\mathrm{card}\left\{\Phi^{(\mathrm{I,2hop})}_{\mathrm{BS}}\right\}}} (1-K_T)\,(P_T/N_{RS})\,\mathcal{Z}^{-1}_{\mathrm{RN_k},\mathrm{MT}_0} \times \left|\mathbf{h}_{\mathrm{RN_k},\mathrm{MT}_0}\mathbf{w}_{\mathrm{RN_k},\mathrm{MT}_0}\right|^2\mathbf{1}\left(\eta_{\mathrm{cell}}\mathcal{Z}_{\mathrm{RN}_k,\mathrm{MT}_0} > \mathcal{Z}_{\mathrm{BS}_0,\mathrm{MT}_0}\right),$$

2) Two-Hop Transmission: In the case that the communication takes place in two hops, RN_0 and $\mathrm{BS_{R0}}$ are defined in (2). In the following, we describe the signal model for each of the two hops.

a) First Hop: Communication between $\mathrm{BS_{R0}}$ *and* RN_0: The received signal at RN_0 from $\mathrm{BS_{R0}}$, which we denote by y_{RN_0}, is given by

$$y_{\mathrm{RN}_0} = \sqrt{\frac{K_T P_T}{N_{BS}\mathcal{Z}_{\mathrm{BS_{R0}RN}_0}}}\mathbf{w}^{Rx}_{\mathrm{BS_{R0}RN}_0}\mathbf{H}_{\mathrm{BS_{R0}RN}_0} \times \mathbf{w}^{Tx}_{\mathrm{BS_{R0}RN}_0}s_{0_n} + \sqrt{(1-K_T)\,(P_T/N_{RS})}\mathbf{w}^{Rx}_{\mathrm{BS_{R0}RN}_0}\mathbf{H}_{\mathrm{SI}}\mathbf{w}_{\mathrm{RN}_0,\mathrm{MT}_0}s'_{0_{n-1}} + i^{(1)}_{\mathrm{BS},\mathrm{RN}_0} + i^{(2)}_{\mathrm{BS},\mathrm{RN}_0} + i_{\mathrm{RN},\mathrm{RN}_0} + n_{\mathrm{RN}_0}, \quad (6)$$

where $\mathbf{H}_{\mathrm{BS_{R0}},\mathrm{RN}_0} \in \mathbb{CN}^{N^{Rx}_{RN}\times N_{BS}}$, $\mathbf{w}^{Tx}_{\mathrm{BS_{R0}RN}_0} \in \mathbb{C}^{N_{BS}\times 1}$ and $\mathbf{w}^{Rx}_{\mathrm{BS_{R0}RN}_0} \in \mathbb{C}^{1\times N^{Rx}_{RN}}$ are the employed beamforming vectors at $\mathrm{BS_{R0}}$ and RN_0, respectively, $\mathbf{w}_{\mathrm{RN}_0,\mathrm{MT}_0} \in \mathbb{C}^{N^{Tx}_{RN}\times 1}$ is the employed beamforming vector at RN_0, $E\left\{n_{\mathrm{RN}_0}n^*_{\mathrm{RN}_0}\right\} = \sigma^2_N$, and $i^{(1)}_{\mathrm{BS},\mathrm{RN}_0}$, $i^{(2)}_{\mathrm{BS},\mathrm{RN}_0}$ are the interference processes affecting RN_0, which result from the BSs constituting the single- and two-hop transmissions, respectively, and given by

$$i^{(1)}_{\mathrm{BS},\mathrm{RN}_0} = \sum_{\mathrm{BS_i}\in\Phi^{(\mathrm{I,1hop})}_{\mathrm{BS}}} \sqrt{(P_T/N_{BS})\,\mathcal{Z}^{-1}_{\mathrm{BS_i},\mathrm{RN}_0}}\mathbf{w}^{Rx}_{\mathrm{BS_{R0}RN}_0}\mathbf{H}_{\mathrm{BS_i},\mathrm{RN}_0}\mathbf{w}_{\mathrm{BS_i},\mathrm{MT_i}}s_{i_n} \mathbf{1}\left(\mathcal{Z}_{\mathrm{BS_i},\mathrm{RN}_0} > \mathcal{Z}_{\mathrm{BS_{R0}},\mathrm{RN}_0}\right)\mathbf{1}\left(\mathcal{Z}_{\mathrm{BS_i},\mathrm{MT}_0} > \eta_{\mathrm{cell}}\mathcal{Z}_{\mathrm{RN}_0,\mathrm{MT}_0}\right)$$

$$i^{(2)}_{\mathrm{BS},\mathrm{RN}_0} = \sum_{\mathrm{BS_j}\in\Phi^{(\mathrm{I,2hop})}_{\mathrm{BS}}} \sqrt{K_T(P_T/N_{BS})\,\mathcal{Z}^{-1}_{\mathrm{BS_j},\mathrm{RN}_0}}\mathbf{w}^{Rx}_{\mathrm{BS_{R0}RN}_0}\mathbf{H}_{\mathrm{BS_j},\mathrm{MT}_0}\mathbf{w}^{Tx}_{\mathrm{BS_j},\mathrm{RN_j}} \times s_{j_n}\mathbf{1}\left(\mathcal{Z}_{\mathrm{BS_j},\mathrm{RN}_0} > \mathcal{Z}_{\mathrm{BS_{R0}},\mathrm{RN}_0}\right)\mathbf{1}\left(\mathcal{Z}_{\mathrm{BS_j},\mathrm{MT}_0} > \eta_{\mathrm{cell}}\mathcal{Z}_{\mathrm{RN}_0,\mathrm{MT}_0}\right),$$

and $i_{\mathrm{RN},\mathrm{RN}_0}$ is the interference process affecting RN_0, which is caused by the set of interfering RNs. It is given by

$$i_{\mathrm{RN},\mathrm{RN}_0} = \sum_{\substack{\mathrm{RN}_k\in\Phi^{(\mathrm{I})}_{\mathrm{RN}} \\ \mathrm{card}\left\{\Phi^{(\mathrm{I})}_{\mathrm{RN}}\right\}=\mathrm{card}\left\{\Phi^{(\mathrm{I,2hop})}_{\mathrm{BS}}\right\}}} \sqrt{(1-K_T)\,(P_T/N_{RS})\,\mathcal{Z}^{-1}_{\mathrm{RN_k},\mathrm{RN}_0}}\mathbf{w}^{Rx}_{\mathrm{BS_{R0}RN}_0} \times \mathbf{H}_{\mathrm{RN_k},\mathrm{RN}_0}\mathbf{w}_{\mathrm{RN_k},\mathrm{MT_k}}s'_{k_{n-1}}\mathbf{1}\left(\mathcal{Z}_{\mathrm{RN}_k,\mathrm{MT}_0} > \mathcal{Z}_{\mathrm{RN}_0,\mathrm{MT}_0}\right).$$

Hence, the resulting from (6) SINR at RN_0, denoted by

$$\mathrm{SINR}_{\mathrm{BS_{R0},RN_0}} = \frac{K_T\left(P_T/N_{BS}\right)\left|\mathbf{w}^{Rx}_{\mathrm{BS_{R0}RN_0}}\mathbf{H}_{\mathrm{BS_{R0},RN_0}}\mathbf{w}^{Tx}_{\mathrm{BS_{R0},RN_0}}\right|^2\mathcal{Z}^{-1}_{\mathrm{BS_{R0},RN_0}}}{\sigma_N^2+\left(1-K_T\right)\left(P_T/N_{RS}\right)\left|\mathbf{w}^{Rx}_{\mathrm{BS_{R0},RN_0}}\mathbf{H}_{\mathrm{SI}}\mathbf{w}_{\mathrm{RN_0,MT_0}}\right|^2+I^{(1)}_{\mathrm{BS,RN_0}}+I^{(2)}_{\mathrm{BS,RN_0}}+I_{\mathrm{RN,RN_0}}} \tag{7}$$

$$\mathrm{SINR}_{\mathrm{RN_0,MT_0}} = \frac{\left(1-K_T\right)\left(P_T/N^{Tx}_{RN}\right)\left|\mathbf{h}_{\mathrm{RN_0,MT_0}}\mathbf{w}_{\mathrm{RN_0,MT_0}}\right|^2\mathcal{Z}^{-1}_{\mathrm{RN_0,MT_0}}}{\sigma_N^2+K_T\left(P_T/N_{BS}\right)\mathcal{Z}^{-1}_{\mathrm{BS_{R0},MT_0}}\left|\mathbf{h}_{\mathrm{BS_{R0},MT_0}}\mathbf{w}^{Tx}_{\mathrm{BS_{R0},RN_0}}\right|^2+\tilde{I}^{(1)}_{\mathrm{BS,MT_0}}+\tilde{I}^{(2)}_{\mathrm{BS,MT_0}}+I^{(2)}_{\mathrm{RN,MT_0}}}, \tag{8}$$

$\mathrm{SINR}_{\mathrm{BS_{R0},RN_0}}$, is given by (7) at the top of the next page, where

$$I^{(1)}_{\mathrm{BS,RN_0}} = \sum_{\mathrm{BS_i}\in\Phi^{(\mathrm{I,1hop})}_{\mathrm{BS}}}\left(P_T/N_{BS}\right)\mathcal{Z}^{-1}_{\mathrm{BS_i,RN_0}}\left|\mathbf{w}^{Rx}_{\mathrm{BS_{R0}RN_0}}\mathbf{H}_{\mathrm{BS_i,RN_0}}\mathbf{w}_{\mathrm{BS_i,MT_i}}\right|^2 \mathbf{1}\left(\mathcal{Z}_{\mathrm{BS_i,RN_0}}>\mathcal{Z}_{\mathrm{BS_{R0},RN_0}}\right)\mathbf{1}\left(\mathcal{Z}_{\mathrm{BS_i,MT_0}}>\eta_{\mathrm{cell}}\mathcal{Z}_{\mathrm{RN_0,MT_0}}\right)$$

$$I^{(2)}_{\mathrm{BS,RN_0}} = \sum_{\mathrm{BS_j}\in\Phi^{(\mathrm{I,2hop})}_{\mathrm{BS}}}K_T(P_T/N_{BS})\,\mathcal{Z}^{-1}_{\mathrm{BS_j,RN_0}}\left|\mathbf{w}^{Rx}_{\mathrm{BS_{R0}RN_0}}\mathbf{H}_{\mathrm{BS_j,MT_0}}\mathbf{w}^{Tx}_{\mathrm{BS_j,RN_j}}\right|^2 \mathbf{1}\left(\mathcal{Z}_{\mathrm{BS_j,RN_0}}>\mathcal{Z}_{\mathrm{BS_{R0},RN_0}}\right)\mathbf{1}\left(\mathcal{Z}_{\mathrm{BS_j,MT_0}}>\eta_{\mathrm{cell}}\mathcal{Z}_{\mathrm{RN_0,MT_0}}\right)$$

and

$$I_{\mathrm{RN,RN_0}} = \sum_{\substack{\mathrm{RN}_k\in\Phi^{(\mathrm{I})}_{\mathrm{RN}}\\ \mathrm{card}\left\{\Phi^{(\mathrm{I})}_{\mathrm{RN}}\right\}=\mathrm{card}\left\{\Phi^{(\mathrm{I,2hop})}_{\mathrm{BS}}\right\}}}\frac{\left(1-K_T\right)P_T}{N_{RS}\mathcal{Z}_{\mathrm{RN}_k,\mathrm{RN_0}}}\left|\mathbf{w}^{Rx}_{\mathrm{BS_{R0}RN_0}}\mathbf{H}_{\mathrm{RN}_k,\mathrm{RN_0}}\mathbf{w}_{\mathrm{RN}_k,\mathrm{MT}_k}\right|^2 \mathbf{1}\left(\mathcal{Z}_{\mathrm{RN}_k,\mathrm{MT_0}}>\mathcal{Z}_{\mathrm{RN_0,MT_0}}\right). \tag{9}$$

b) Second Hop: In the second hop, the received signal at MT_0, denoted by $y^{(2)}_{\mathrm{MT_0}}$, is given by

$$y^{(2)}_{\mathrm{MT_0}} = \sqrt{\left(1-K_T\right)\left(P_T/N_{RS}\right)\mathcal{Z}^{-1}_{\mathrm{RN_0,MT_0}}}\mathbf{h}_{\mathrm{RN_0,MT_0}}\mathbf{w}_{\mathrm{RN_0,MT_0}}s'_{0_n} + \sqrt{K_T\left(P_T/N_{BS}\right)\mathcal{Z}^{-1}_{\mathrm{BS_{R0},MT_0}}}\mathbf{h}_{\mathrm{BS_{R0},MT_0}}\mathbf{w}^{Tx}_{\mathrm{BS_{R0},RN_0}}s_{0_{n+1}} + \tilde{i}^{(1)}_{\mathrm{BS,MT_0}}+\tilde{i}^{(2)}_{\mathrm{BS,MT_0}}+i^{(2)}_{\mathrm{RN,MT_0}}+n^{(2)}_{\mathrm{MT_0}}, \tag{10}$$

where $\mathbf{h}_{\mathrm{RN_0,MT_0}}\in\mathbb{CN}^{1\times N^{Tx}_{RN}}$, $E\left\{n^{(2)}_{\mathrm{MT_0}}n^{(2)*}_{\mathrm{MT_0}}\right\}=\sigma_N^2$, $\sqrt{K_T\left(P_T/N_{BS}\right)\mathcal{Z}^{-1}_{\mathrm{BS_{R0},MT_0}}}\mathbf{h}_{\mathrm{BS_{R0},MT_0}}\mathbf{w}_{\mathrm{BS_{R0},RN_0}}$ is the interfering signal from $\mathrm{BS_{R0}}$ towards MT_0. $\tilde{i}^{(1)}_{\mathrm{BS,MT_0}}$ and $\tilde{i}^{(2)}_{\mathrm{BS,MT_0}}$ are the interference processes affecting MT_0, which result from the set of BSs constituting the single- and two-hop transmissions, respectively. They are given by

$$\tilde{i}^{(1)}_{\mathrm{BS,MT_0}} = \sum_{\mathrm{BS_i}\in\Phi^{(\mathrm{I,1hop})}_{\mathrm{BS}}}\sqrt{\left(P_T/N_{BS}\right)\mathcal{Z}^{-1}_{\mathrm{BS_i,RN_0}}}\mathbf{h}_{\mathrm{BS_i,MT_0}}\mathbf{w}_{\mathrm{BS_i,MT_i}}s_{i_{n+1}} \mathbf{1}\left(\mathcal{Z}_{\mathrm{BS_i,RN_0}}>\mathcal{Z}_{\mathrm{BS_{R0},RN_0}}\right)\mathbf{1}\left(\mathcal{Z}_{\mathrm{BS_i,MT_0}}>\eta_{\mathrm{cell}}\mathcal{Z}_{\mathrm{RN_0,MT_0}}\right), \tag{11}$$

$$\tilde{i}^{(2)}_{\mathrm{BS,MT_0}} = \sum_{\mathrm{BS_j}\in\Phi^{(\mathrm{I,2hop})}_{\mathrm{BS}}}\sqrt{K_T(P_T/N_{BS})\,\mathcal{Z}^{-1}_{\mathrm{BS_j,MT_0}}}\mathbf{h}_{\mathrm{BS_j,MT_0}}\mathbf{w}^{Tx}_{\mathrm{BS_j,RN_j}}s_{j_{n+1}} \mathbf{1}\left(\mathcal{Z}_{\mathrm{BS_j,RN_0}}>\mathcal{Z}_{\mathrm{BS_{R0},RN_0}}\right)\mathbf{1}\left(\mathcal{Z}_{\mathrm{BS_j,MT_0}}>\eta_{\mathrm{cell}}\mathcal{Z}_{\mathrm{RN_0,MT_0}}\right), \tag{12}$$

and

$$i^{(2)}_{\mathrm{RN,MT_0}} = \sum_{\substack{\mathrm{RN}_k\in\Phi^{(\mathrm{I})}_{\mathrm{RN}}\\ \mathrm{card}\left\{\Phi^{(\mathrm{I})}_{\mathrm{RN}}\right\}=\mathrm{card}\left\{\Phi^{(\mathrm{I,2hop})}_{\mathrm{BS}}\right\}}}\sqrt{\left(1-K_T\right)\left(P_T/N_{RS}\right)\mathcal{Z}^{-1}_{\mathrm{RN}_k,\mathrm{MT_0}}}\mathbf{h}_{\mathrm{RN}_k,\mathrm{MT_0}} \times\mathbf{w}_{\mathrm{RN}_k,\mathrm{MT_0}}s'_{k_n}\mathbf{1}\left(\mathcal{Z}_{\mathrm{RN}_k,\mathrm{MT_0}}>\mathcal{Z}_{\mathrm{RN_0,MT_0}}\right). \tag{13}$$

Consequently, based on (10), the SINR at MT_0, denoted by $\mathrm{SINR}_{\mathrm{RN_0,MT_0}}$, is given by (8) at the top of the page, where

$$\tilde{I}^{(1)}_{\mathrm{BS,MT_0}} = \sum_{\mathrm{BS_i}\in\Phi^{(\mathrm{I,1hop})}_{\mathrm{BS}}}\left(P_T/N_{BS}\right)\mathcal{Z}^{-1}_{\mathrm{BS_i,MT_0}}\left|\mathbf{h}_{\mathrm{BS_i,MT_0}}\mathbf{w}_{\mathrm{BS_i,MT_i}}\right|^2 \mathbf{1}\left(\mathcal{Z}_{\mathrm{BS_i,RN_0}}>\mathcal{Z}_{\mathrm{BS_{R0},RN_0}}\right)\mathbf{1}\left(\mathcal{Z}_{\mathrm{BS_i,MT_0}}>\eta_{\mathrm{cell}}\mathcal{Z}_{\mathrm{RN_0,MT_0}}\right), \tag{14}$$

$$\tilde{I}^{(2)}_{\mathrm{BS,MT_0}} = \sum_{\mathrm{BS_j}\in\Phi^{(\mathrm{I,2hop})}_{\mathrm{BS}}}K_T(P_T/N_{BS})\,\mathcal{Z}^{-1}_{\mathrm{BS_j,MT_0}}\left|\mathbf{h}_{\mathrm{BS_j,MT_0}}\mathbf{w}^{Tx}_{\mathrm{BS_j,RN_j}}\right|^2 \mathbf{1}\left(\mathcal{Z}_{\mathrm{BS_j,RN_0}}>\mathcal{Z}_{\mathrm{BS_{R0},RN_0}}\right)\mathbf{1}\left(\mathcal{Z}_{\mathrm{BS_j,MT_0}}>\eta_{\mathrm{cell}}\mathcal{Z}_{\mathrm{RN_0,MT_0}}\right), \tag{15}$$

and

$$I^{(2)}_{\mathrm{RN,MT_0}} = \sum_{\substack{\mathrm{RN}_k\in\Phi^{(\mathrm{I})}_{\mathrm{RN}}\\ \mathrm{card}\left\{\Phi^{(\mathrm{I})}_{\mathrm{RN}}\right\}=\mathrm{card}\left\{\Phi^{(\mathrm{I,2hop})}_{\mathrm{BS}}\right\}}}\left(1-K_T\right)\left(P_T/N^{Tx}_{RN}\right)\left|\mathbf{h}_{\mathrm{RN}_k,\mathrm{MT_0}}\mathrm{w}_{\mathrm{RN}_k,\mathrm{MT_0}}\right|^2 \times\mathcal{Z}^{-1}_{\mathrm{RN}_k,\mathrm{MT_0}}\mathbf{1}\left(\mathcal{Z}_{\mathrm{RN}_k,\mathrm{MT_0}}>\mathcal{Z}_{\mathrm{RN_0,MT_0}}\right).$$

c) Design of $\mathbf{w}_{\mathrm{RN_0,MT_0}}$, $\mathbf{w}^{Tx}_{\mathrm{BS_{R0},RN_0}}$, and $\mathbf{w}^{Rx}_{\mathrm{BS_{R0},RN_0}}$: Owing to the expected relatively small distance between $\mathrm{BS_{R0}}$ and MT_0, according to the cell-association criterion of (2), the statistical power effect of the interference term $K_T\left(P_T/N_{BS}\right)\mathcal{Z}^{-1}_{\mathrm{BS_{R0},MT_0}}\left|\mathbf{h}_{\mathrm{BS_{R0},MT_0}}\mathbf{w}^{Tx}_{\mathrm{BS_{R0},RN_0}}\right|^2$, which is involved in the first hop, is expected to be strong. Due to this, propose the design of $\mathbf{w}_{\mathrm{RN_0,MT_0}}$, $\mathbf{w}^{Tx}_{\mathrm{BS_{R0},RN_0}}$, and $\mathbf{w}^{Rx}_{\mathrm{BS_{R0},RN_0}}$ with the aim of canceling it, while at the same time maximizing the useful signal terms $\left|\mathbf{w}^{Rx}_{\mathrm{BS_{R0},RN_0}}\mathbf{H}_{\mathrm{BS_{R0},RN_0}}\mathbf{w}^{Tx}_{\mathrm{BS_{R0}RN_0}}\right|^2$ and $\left|\mathbf{h}_{\mathrm{RN_0,MT_0}}\mathbf{w}_{\mathrm{RN_0,MT_0}}\right|^2$ of (7) and (8), respectively. Hence, according to the MRT principle it holds that $\mathbf{w}_{\mathrm{RN_0,MT_0}}=\frac{\mathbf{h}^H_{\mathrm{RN_0,MT_0}}}{\left\|\mathbf{h}^H_{\mathrm{RN_0,MT_0}}\right\|}$ and regarding $\mathbf{w}^{Tx}_{\mathrm{BS_{R0},RN_0}}$ and $\mathbf{w}^{Rx}_{\mathrm{BS_{R0},RN_0}}$ the optimization problem to be solved is:

$$\begin{aligned}\max_{\mathbf{w}^{Rx}_{\mathrm{BS_{R0},RN_0}},\mathbf{w}^{Tx}_{\mathrm{BS_{R0},RN_0}}}\quad&\left|\mathbf{w}^{Rx}_{\mathrm{BS_{R0}RN_0}}\mathbf{H}_{\mathrm{BS_{R0}RN_0}}\mathbf{w}^{Tx}_{\mathrm{BS_{R0}RN_0}}\right|^2\\ \text{s.t.}\quad&\left|\mathbf{h}_{\mathrm{BS_{R0},MT_0}}\mathbf{w}^{Tx}_{\mathrm{BS_{R0},RN_0}}\right|^2=0.\end{aligned} \tag{16}$$

Proposition 1. *If $N_{BS}>1$, the solution of* (16) *is given by*

$$\begin{aligned}\mathbf{w}^{Rx}_{\mathrm{BS_{R0},RN_0}}&=\mathbf{u}^{(l)}_{\mathrm{BS_{R0},RN_0}}\\ \mathbf{w}^{Tx}_{\mathrm{BS_{R0},RN_0}}&=\frac{\mathbf{P}_{\mathbf{h}_{\mathrm{BS_{R0},MT_0}}}\mathbf{u}^{(r)}_{\mathrm{BS_{R0},RN_0}}}{\left\|\mathbf{P}_{\mathbf{h}_{\mathrm{BS_{R0},MT_0}}}\mathbf{u}^{(r)}_{\mathrm{BS_{R0},RN_0}}\right\|},\end{aligned} \tag{17}$$

where $\mathbf{u}^{(l)}_{\mathrm{BS_{R0},RN_0}}$ and $\mathbf{u}^{(r)}_{\mathrm{BS_{R0},RN_0}}$ are the left and right singular vectors that correspond to the largest singular value

of $\mathbf{H}_{\mathrm{BS_{R0},RN_0}}$ *and*

$$\mathbf{P}_{\mathbf{h}_{\mathrm{BS_{R0},MT_0}}} = \mathbf{I}_{N_{BS}} - \mathbf{h}^{H}_{\mathrm{BS_{R0},MT_0}} \left(\mathbf{h}_{\mathrm{BS_{R0},MT_0}} \mathbf{h}^{H}_{\mathrm{BS_{R0},MT_0}}\right)^{-1} \times \mathbf{h}_{\mathrm{BS_{R0},MT_0}}. \quad (18)$$

Proof*: To satisfy* (16)*,* $\mathbf{w}^{Tx}_{\mathrm{BS_{R0},RN_0}}$ *needs to be in the orthogonal complement space of* $\mathbf{h}_{\mathrm{BS_{R0},MT_0}}$ *and at the same time together with* $\mathbf{w}^{Rx}_{\mathrm{BS_{R0},RN_0}}$ *to maximize* $\left|\mathbf{w}^{Rx}_{\mathrm{BS_{R0}RN_0}} \mathbf{H}_{\mathrm{BS_{R0}RN_0}} \mathbf{w}^{Tx}_{\mathrm{BS_{R0}RN_0}}\right|^2$*. Hence,* (16) *admits the solution of* (17) *with* $\mathbf{P}_{\mathbf{h}_{\mathrm{BS_{R0},MT_0}}} \in \mathbb{C}^{N_{BS}\times N_{BS}}$ *being the orthogonal projection onto the orthogonal complement of the column space of* $\mathbf{h}_{\mathrm{BS_{R0},MT_0}}$.

Remark 1. (16) *does not admit a solution when* $N_{BS} = 1$ *and, consequently, the interference term* $K_T\left(P_T/N_{BS}\right)\mathcal{Z}^{-1}_{\mathrm{BS_{R0},MT_0}} \left|\mathbf{h}_{\mathrm{BS_{R0},MT_0}} \mathbf{w}^{Tx}_{\mathrm{BS_{R0},RN_0}}\right|^2$ *cannot be eliminated. For simplification of the analysis in Section IV and in order to observe the maximum performance that can be attained by using FD RNs, in the rest of this paper we assume that* $N_{BS} > 1$ *and, hence,* (16) *admits the solution of* (17) *according to which* $\left|\mathbf{h}_{\mathrm{BS_{R0},MT_0}} \mathbf{w}^{Tx}_{\mathrm{BS_{R0},RN_0}}\right|^2 = 0$.

B. Examined Performance Metric

In this work, we consider the xth percentile rate of $\mathrm{MT_0}$ as the performance metric of interest. It is the rate threshold for which the probability that the instantaneous rate $\mathrm{B_W}\log_2\left(1+\mathrm{SINR}\right)$ is smaller than that threshold is $\mathrm{x}\%$. To mathematically define it, it is convenient to first define the coverage probability, which is the probability that the SINR at $\mathrm{MT_0}$ in a single-hop transmission or at both $\mathrm{RN_0}$ and $\mathrm{MT_0}$ in a two-hop transmission is greater than a particular threshold. By defining it as $\mathrm{P_{cov}}\left(\mathrm{T}\right)$, where T is the threshold, it is given by

$$\mathrm{P_{cov}}\left(\mathrm{T}\right) = \mathbb{E}_{\mathcal{Z}_{\mathrm{BS_0,MT_0}}}\left\{\mathrm{P}^{(\mathrm{1hop})}_{\mathrm{cov}}\left(\mathrm{T};\mathcal{Z}_{\mathrm{BS_0,MT_0}}\right)\right\} + \mathbb{E}_{\mathcal{Z}_{\mathrm{RN_0,MT_0}}}\left\{\mathrm{P}^{(\mathrm{2hop})}_{\mathrm{cov}}\left(\mathrm{T};\mathcal{Z}_{\mathrm{RN_0,MT_0}}\right)\right\}, \quad (19)$$

where $\mathrm{P}^{(\mathrm{1hop})}_{\mathrm{cov}}\left(\cdot;\cdot\right)$, $\mathrm{P}^{(\mathrm{2hop})}_{\mathrm{cov}}\left(\cdot;\cdot\right)$ are the coverage probabilities corresponding to one- and two-hop links, respectively. They are given by (20) at the top of the next page. The xth percentile rate, which we denote by $\mathrm{R_{xth}}$, is given by the solution of the following equation:

$$\Pr\left\{\mathrm{B_W}\log_2\left(1+\mathrm{SINR}\right) < \mathrm{R_{xth}}\right\} = \mathrm{xth} \Rightarrow 1-\mathrm{P_{cov}}\left(2^{\frac{\mathrm{R_{xth}}}{\mathrm{B_w}}}-1\right) = \mathrm{xth}, \quad (23)$$

where $\mathrm{P_{cov}}\left(\cdot\right)$ is given by (19).

IV. Performance Analysis

In this section, we derive the analytical expression of $\mathrm{R_{xth}}$. Towards this, i) At first, we present the analytical expressions of the required distributions to derive this expression. ii) We consider useful geometrical approximations for tractability.

A. Preliminaries

It is evident from Section III-B that the derivation of the analytical expression of $\mathrm{R_{xth}}$ requires the computation of the following quantities: i) The distribution and the pdf of $\mathcal{Z}_{X_0,Y_0} = l\left(r_{X_0,Y_0}\right)/S_{X_0,Y_0}$, which we denote by $F_{\mathcal{Z}_{X_0,Y_0}}\left(\cdot\right)$ and $f_{\mathcal{Z}_{X_0,Y_0}}\left(\cdot\right)$, respectively. They are given by [38, Eq. (31)]

$$F_{\mathcal{Z}_{X_0,Y_0}}\left(x\right) = 1 - \exp\left(-\pi\lambda_X \kappa_0^{-2/\beta_{X,Y_0}} \Upsilon_{X,Y_0} x^{2/\beta_{X,Y_0}}\right) \quad (24)$$

$$f_{\mathcal{Z}_{X_0,Y_0}}\left(\xi\right) = \left(2\pi\lambda_X \kappa_0^{-2/\beta_{X,Y_0}} \Upsilon_{X,Y_0} \xi^{2/\beta_{X,Y_0}-1} \Big/ \beta_{X,Y_0}\right) \times \exp\left(-\pi\lambda_X \kappa_0^{-2/\beta_{X,Y_0}} \Upsilon_{X,Y_0} \xi^{2/\beta_{X,Y_0}}\right), \quad (25)$$

where

$$\Upsilon_{X,Y_0} = \exp\left(G_{X,Y_0}\mu_{X,Y_0} + \frac{1}{2}G^2_{X,Y_0}\sigma^2_{X,Y_0}\right) \quad (26)$$

with $G_{X,Y_0} = \frac{1}{10\log_{10}(e)}\frac{2}{\beta_{X,Y_0}}$. ii) The conditional probabilities that $\mathrm{MT_0}$ is served via a one-hop and a two-hop link, i.e.

$$\chi_{\mathrm{1hop}}\left(\mathcal{Z}_{\mathrm{BS_0,MT_0}}\right) = \Pr\left\{\mathcal{Z}_{\mathrm{RN_0,MT_0}} \geq \eta^{-1}_{\mathrm{cell}}\mathcal{Z}_{\mathrm{BS_0,MT_0}} \middle|\, \mathcal{Z}_{\mathrm{BS_0,MT_0}}\right\} = 1 - F_{\mathcal{Z}_{\mathrm{RN_0,MT_0}}}\left(\eta^{-1}_{\mathrm{cell}}\mathcal{Z}_{\mathrm{BS_0,MT_0}}\right) \quad (27)$$

$$\chi_{\mathrm{2hop}}\left(\mathcal{Z}_{\mathrm{RN_0,MT_0}}\right) = \Pr\left\{\mathcal{Z}_{\mathrm{BS_0,MT_0}} > \eta_{\mathrm{cell}}\mathcal{Z}_{\mathrm{RN_0,MT_0}} \middle|\, \mathcal{Z}_{\mathrm{RN_0,MT_0}}\right\} = 1 - F_{\mathcal{Z}_{\mathrm{BS_0,MT_0}}}\left(\eta_{\mathrm{cell}}\mathcal{Z}_{\mathrm{RN_0,MT_0}}\right). \quad (28)$$

iii) The probabilities that $\mathrm{MT_0}$ is served via a one- and a two-hop link, *i.e.*, χ_{1hop} and χ_{2hop}. χ_{1hop} are given by

$$\chi_{\mathrm{1hop}} = \int_0^{+\infty}\left(1 - F_{\mathcal{Z}_{\mathrm{RN_0,MT_0}}}\left(\eta^{-1}_{\mathrm{cell}}\xi\right)\right) f_{\mathcal{Z}_{\mathrm{BS_0,MT_0}}}\left(\xi\right) d\xi \quad (29)$$

and χ_{2hop}=1-χ_{1hop}.

B. Approximations

Approximation 1. *For analytical tractability, we propose to approximate* $\mathrm{SINR_{BS_{R0},RN_0}}$*, defined in* (7)*, as as* (21) *at the top of the next page, where*

$$I^{approx(1)}_{\mathrm{BS,RN_0}} \approx \sum_{\mathrm{BS_i}\in\Phi^{(\mathrm{I,1hop})}_{\mathrm{BS}}} \frac{P_T}{N_{BS}\mathcal{Z}_{\mathrm{BS_i,RN_0}}} \left|\mathbf{w}^{Rx}_{\mathrm{BS_{R0}RN_0}} \mathbf{H}_{\mathrm{BS_i,RN_0}} \mathbf{w}_{\mathrm{BS_i,MT_i}}\right|^2 \mathbf{1}\left(\mathcal{Z}_{\mathrm{BS_i,RN_0}} > \mathcal{Z}_{\mathrm{BS_{R0},RN_0}}\right), \quad (30)$$

$$I^{approx(2)}_{\mathrm{BS,RN_0}} \approx \sum_{\mathrm{BS_j}\in\Phi^{(\mathrm{I,2hop})}_{\mathrm{BS}}} \frac{K_T P_T}{N_{BS}\mathcal{Z}_{\mathrm{BS_j,RN_0}}} \left|\mathbf{w}^{Rx}_{\mathrm{BS_{R0}RN_0}} \mathbf{H}_{\mathrm{BS_j,MT_0}} \mathbf{w}^{Tx}_{\mathrm{BS_j,RN_j}}\right|^2 \mathbf{1}\left(\mathcal{Z}_{\mathrm{BS_j,RN_0}} > \mathcal{Z}_{\mathrm{BS_{R0},RN_0}}\right), \quad (31)$$

and

$$I^{approx}_{\mathrm{RN,RN_0}} \approx \sum_{\substack{\mathrm{RN_k}\in\Phi^{(\mathrm{I})}_{\mathrm{RN}} \\ \mathrm{card}\left\{\Phi^{(\mathrm{I})}_{\mathrm{RN}}\right\}=\mathrm{card}\left\{\Phi^{(\mathrm{I,2hop})}_{\mathrm{BS}}\right\}}} \frac{\left(1-K_T\right)P_T}{N^{Tx}_{RN}\mathcal{Z}_{\mathrm{RN_k,RN_0}}} \left|\mathbf{h}_{\mathrm{RN_k,RN_0}} \mathbf{w}_{\mathrm{RN_k,MT_k}}\right|^2. \quad (32)$$

Remark 2. (30) *and* (31) *occur by not taking into account the indicator functions* $\mathbf{1}\left(\mathcal{Z}_{\mathrm{BS}_i,\mathrm{MT}_0} > \eta_{\mathrm{cell}}\mathcal{Z}_{\mathrm{RN_0,MT_0}}\right)$ *and* $\mathbf{1}\left(\mathcal{Z}_{\mathrm{BS_j,MT_0}} > \eta_{\mathrm{cell}}\mathcal{Z}_{\mathrm{RN_0,MT_0}}\right)$ *in* (9)*. By considering that the communication takes place in two hops and by excluding shadowing for simplicity, such an approximation restricts the interfering BSs of* RN_0*, related to the single- and two-hop transmissions, to the area that lies outside the disc with center* RN_0 *and radius equal to* $r_{\mathrm{BS_{R0},RN_0}}$ *(Fig. 1). Such an assumption is expected to hold reasonably well for RN*

$$\begin{aligned}\mathrm{P}_{\mathrm{cov}}^{(1\mathrm{hop})}\left(\mathrm{T};\mathcal{Z}_{\mathrm{BS}_0,\mathrm{MT}_0}\right)&=\Pr\left\{\mathrm{SINR}_{\mathrm{BS}_0,\mathrm{MT}_0}>\mathrm{T}\middle|\,\mathcal{Z}_{\mathrm{BS}_0,\mathrm{MT}_0}\right\}\Pr\left\{\mathcal{Z}_{\mathrm{RN}_0,\mathrm{MT}_0}\geq\eta_{\mathrm{cell}}^{-1}\mathcal{Z}_{\mathrm{BS}_0,\mathrm{MT}_0}\middle|\,\mathcal{Z}_{\mathrm{BS}_0,\mathrm{MT}_0}\right\}\\ \mathrm{P}_{\mathrm{cov}}^{(2\mathrm{hop})}\left(\mathrm{T};\mathcal{Z}_{\mathrm{RN}_0,\mathrm{MT}_0}\right)&=\Pr\left\{\mathrm{SINR}_{\mathrm{BS}_{\mathrm{R}0},\mathrm{RN}_0}>\mathrm{T}\text{ and }\mathrm{SINR}_{\mathrm{RN}_0,\mathrm{MT}_0}>\mathrm{T}\middle|\,\mathcal{Z}_{\mathrm{RN}_0,\mathrm{MT}_0}\right\}\\ &\quad\times\Pr\left\{\mathcal{Z}_{\mathrm{BS}_0,\mathrm{MT}_0}>\eta_{\mathrm{cell}}\mathcal{Z}_{\mathrm{RN}_0,\mathrm{MT}_0}\middle|\,\mathcal{Z}_{\mathrm{RN}_0,\mathrm{MT}_0}\right\}.\end{aligned}\tag{20}$$

$$\mathrm{SINR}_{\mathrm{BS}_{\mathrm{R}0},\mathrm{RN}_0}^{approx}=\frac{K_T\left(P_T/N_{BS}\right)\left|\mathbf{w}_{\mathrm{BS}_{\mathrm{R}0}\mathrm{RN}_0}^{Rx}\mathbf{H}_{\mathrm{BS}_{\mathrm{R}0},\mathrm{RN}_0}\mathbf{w}_{\mathrm{BS}_{\mathrm{R}0},\mathrm{RN}_0}^{Tx}\right|^2\mathcal{Z}_{\mathrm{BS}_{\mathrm{R}0},\mathrm{RN}_0}^{-1}}{\sigma_N^2+\left(1-K_T\right)\left(P_T/N_{RN}^{Tx}\right)\left|\mathbf{w}_{\mathrm{BS}_{\mathrm{R}0},\mathrm{RN}_0}^{Rx}\mathbf{H}_{\mathrm{SI}}\mathbf{w}_{\mathrm{RN}_0,\mathrm{MT}_0}\right|^2+I_{\mathrm{BS},\mathrm{RN}_0}^{approx(1)}+I_{\mathrm{BS},\mathrm{RN}_0}^{approx(2)}+I_{\mathrm{RN},\mathrm{RN}_0}^{approx}},\tag{21}$$

$$\mathrm{SINR}_{\mathrm{RN}_0,\mathrm{MT}_0}^{approx}\approx\frac{\left(1-K_T\right)\left(P_T/N_{RN}^{Tx}\right)\left|\mathbf{h}_{\mathrm{RN}_0,\mathrm{MT}_0}\mathbf{w}_{\mathrm{RN}_0,\mathrm{MT}_0}\right|^2\mathcal{Z}_{\mathrm{RN}_0,\mathrm{MT}_0}^{-1}}{\sigma_N^2+\tilde{I}_{\mathrm{BS},\mathrm{MT}_0}^{approx(1)}+\tilde{I}_{\mathrm{BS},\mathrm{MT}_0}^{approx(2)}+I_{\mathrm{RN},\mathrm{MT}_0}^{(2)}},\tag{22}$$

densities notably higher than the ones of the BSs since then $r_{\mathrm{RN}_0,\mathrm{MT}_0}$ *tends to be small.*

(32) *occurs by not taking into account the indicator function* $\mathbf{1}\left(\mathcal{Z}_{\mathrm{RN}_k,\mathrm{MT}_0}>\mathcal{Z}_{\mathrm{RN}_0,\mathrm{MT}_0}\right)$ *of* (9)*. This means that the interferers related to* $I_{\mathrm{RN},\mathrm{RN}_0}^{approx}$ *can be located in the whole dimensional plane. As with the indicator functions* $\mathbf{1}\left(\mathcal{Z}_{\mathrm{BS}_i,\mathrm{MT}_0}>\eta_{\mathrm{cell}}\mathcal{Z}_{\mathrm{RN}_0,\mathrm{MT}_0}\right)$ *and* $\mathbf{1}\left(\mathcal{Z}_{\mathrm{BS}_\mathrm{j},\mathrm{MT}_0}>\eta_{\mathrm{cell}}\mathcal{Z}_{\mathrm{RN}_0,\mathrm{MT}_0}\right)$*, the elimination of* $\mathbf{1}\left(\mathcal{Z}_{\mathrm{RN}_k,\mathrm{MT}_0}>\mathcal{Z}_{\mathrm{RN}_0,\mathrm{MT}_0}\right)$ *is expected to hold reasonably well as an assumption for RN densities notably higher than the corresponding ones of the BSs.*

Approximation 2. *We propose to approximate* $\mathrm{SINR}_{\mathrm{RN}_0,\mathrm{MT}_0}$*, defined in* (8)*, as* (22) *at the top of the next page, where*

$$\tilde{I}_{\mathrm{BS},\mathrm{MT}_0}^{approx(1)}=\sum_{\mathrm{BS_i}\in\Phi_{\mathrm{BS}}^{(\mathrm{I},1\mathrm{hop})}}\left(P_T/N_{BS}\right)\mathcal{Z}_{\mathrm{BS_i},\mathrm{RN}_0}^{-1}\left|\mathbf{h}_{\mathrm{BS_i},\mathrm{MT}_0}\mathbf{w}_{\mathrm{BS_i},\mathrm{MT_i}}\right|^2\mathbf{1}\left(\mathcal{Z}_{\mathrm{BS_i},\mathrm{MT}_0}>\eta_{\mathrm{cell}}\mathcal{Z}_{\mathrm{RN}_0,\mathrm{MT}_0}\right)\tag{33}$$

and

$$\tilde{I}_{\mathrm{BS},\mathrm{MT}_0}^{approx(2)}=\sum_{\mathrm{BS_j}\in\Phi_{\mathrm{BS}}^{(\mathrm{I},2\mathrm{hop})}}K_T(P_T/N_{BS})\,\mathcal{Z}_{\mathrm{BS_j},\mathrm{MT}_0}^{-1}\left|\mathbf{h}_{\mathrm{BS_j},\mathrm{MT}_0}\mathbf{w}_{\mathrm{BS_j},\mathrm{RN_j}}^{Tx}\right|^2\mathbf{1}\left(\mathcal{Z}_{\mathrm{BS_j},\mathrm{MT}_0}>\eta_{\mathrm{cell}}\mathcal{Z}_{\mathrm{RN}_0,\mathrm{MT}_0}\right).\tag{34}$$

Remark 3. (33) *and* (34) *occur by not taking into account the indicator functions* $\mathbf{1}\left(\mathcal{Z}_{\mathrm{BS_i},\mathrm{RN}_0}>\mathcal{Z}_{\mathrm{BS}_{\mathrm{R}0},\mathrm{RN}_0}\right)$ *and* $\mathbf{1}\left(\mathcal{Z}_{\mathrm{BS_j},\mathrm{RN}_0}>\mathcal{Z}_{\mathrm{BS}_{\mathrm{R}0},\mathrm{RN}_0}\right)$ *in* (14) *and* (15)*, respectively. Such approximations originate by using similar arguments as in Remark 2.*

C. Coverage Probability

In this section, we provide a tractable mathematical framework for the computation of $\mathrm{P}_{\mathrm{cov}}\left(\mathrm{T}\right)$, which is used for the computation of $\mathrm{R}_{\mathrm{xth}}$ according to (23). For analytical tractability and to obtain important insights we consider the case of $N_{RN}^{Rx}=1$ and in Section VI we provide simulation results also for the $N_{RN}^{Rx}>1$ case which exhibit the same trends with the $N_{RN}^{Rx}=1$ case. Now, we present Lemma 1 that is used for proving Proposition 2 that is subsequently presented.

Lemma 1. *For* $N_{RN}^{Rx}=1$ *and according to the design of* (17)*,* $\left|\mathbf{w}_{\mathrm{BS}_{\mathrm{R}0}\mathrm{RN}_0}^{Rx}\mathbf{H}_{\mathrm{BS}_{\mathrm{R}0},\mathrm{RN}_0}\mathbf{w}_{\mathrm{BS}_{\mathrm{R}0},\mathrm{RN}_0}^{Tx}\right|^2$ *follows a chi-squared distribution with* $N_{BS}-1$ *degrees of freedom.*

Proof: See the APPENDIX.

Proposition 2. $\mathrm{P}_{\mathrm{cov}}\left(\mathrm{T}\right)$*, defined in* (19)*, can be approximated as*

$$\begin{aligned}\mathrm{P}_{\mathrm{cov}}\left(\mathrm{T}\right)&=\mathbb{E}_{\mathcal{Z}_{\mathrm{BS}_0,\mathrm{MT}_0}}\left\{\mathrm{P}_{\mathrm{cov}}^{(1\mathrm{hop})}\left(\mathrm{T};\mathcal{Z}_{\mathrm{BS}_0,\mathrm{MT}_0}\right)\right\}\\ &\quad+\mathbb{E}_{\mathcal{Z}_{\mathrm{RN}_0,\mathrm{MT}_0}}\left\{\mathrm{P}_{\mathrm{cov}}^{(2\mathrm{hop})}\left(\mathrm{T};\mathcal{Z}_{\mathrm{RN}_0,\mathrm{MT}_0}\right)\right\}\\ &\approx\mathcal{J}_{\mathrm{BS,MT}}\left(\mathrm{T}\right)+\mathcal{J}_{\mathrm{BS,RN}}\left(\mathrm{T}\right)\mathcal{J}_{\mathrm{RN,MT}}\left(\mathrm{T}\right),\end{aligned}\tag{35}$$

where $\mathcal{J}_{\mathrm{BS,MT}}\left(\mathrm{T}\right)$*,* $\mathcal{J}_{\mathrm{BS,RN}}\left(\mathrm{T}\right)$*, and* $\mathcal{J}_{\mathrm{RN,MT}}\left(\mathrm{T}\right)$ *are given by* (36)*,* (37)*, and* (38)*, respectively, on the next page,*

$$p_{\mathrm{X,Y}}^{(k)}\left(\mathrm{y}\right)=\begin{cases}\exp\left(g_{\mathrm{X,Y}}\left(\mathrm{y}\right)\right), & k=0\\ \exp\left(g_{\mathrm{X,Y}}\left(\mathrm{y}\right)\right)\sum\dfrac{k!}{p_1!...p_k!}\left(\dfrac{g_{\mathrm{X,Y}}^{(1)}\left(\mathrm{y}\right)}{1!}\right)^{p_1}\\ \qquad\times...\times\left(\dfrac{g_{\mathrm{X,Y}}^{(k)}\left(\mathrm{y}\right)}{k!}\right)^{p_k}, & k\geq1,\end{cases}\tag{39}$$

where $p_1,...p_k$ *are given by the non-negative integer solutions of the equation*[4] $p_1+2p_2+...kp_k=k$*,* $a_{\mathrm{BS,RN}}=\frac{1-K_T}{K_T}\frac{N_{BS}}{N_{RN}^{Tx}}\mathrm{T}$*,* $\mathrm{X,Y}=\{\left(\mathrm{BS,MT}\right),\left(\mathrm{BS,RN}\right),\left(\mathrm{RN,MT}\right)\}$*, and*

$$\begin{aligned}g_{\mathrm{X,Y}}\left(\mathrm{y}\right)&=B_{\mathrm{X,Y}}\mathrm{y}+C_{\mathrm{X,Y}}\mathrm{y}^{\frac{\beta_{\mathrm{X,Y}}}{\beta_{\bar{\mathrm{X}},\bar{\mathrm{Y}}}}}\\ g_{\mathrm{X,Y}}^{(k)}\left(\mathrm{y}\right)&=g_{\mathrm{X,Y}}\left(\mathrm{y}\right)\prod_{m=1}^{k}\left(\frac{2}{\beta_{\mathrm{X,Y}}}-(m-1)\right)\left(\kappa_0\right)^{-m}\mathrm{y}^{-m\frac{\beta_{\mathrm{X,Y}}}{2}}\end{aligned}\tag{40}$$

with $\bar{\mathrm{X}},\bar{\mathrm{Y}}=\{\left(\mathrm{RN,MT}\right),\left(\mathrm{RN,RN}\right),\left(\mathrm{BS,MT}\right)\}$ if $\mathrm{X,Y}=\{\left(\mathrm{BS,MT}\right),\left(\mathrm{BS,RN}\right),\left(\mathrm{RN,MT}\right)\}$, respectively,

$$\begin{aligned}B_{\mathrm{BS,MT}}&=\pi\lambda_{\mathrm{BS}}^{(\mathrm{I},1\mathrm{hop})}\Upsilon_{\mathrm{BS,MT}}\Psi_{\mathrm{BS,MT}}\left(-\mathrm{T}\right)\\ &\quad+\pi\lambda_{\mathrm{BS}}^{(\mathrm{I},2\mathrm{hop})}\Upsilon_{\mathrm{BS,MT}}\Psi_{\mathrm{BS,MT}}\left(-K_T\mathrm{T}\right)\\ B_{\mathrm{BS,RN}}&=\pi\lambda_{\mathrm{BS}}^{(\mathrm{I},1\mathrm{hop})}\Upsilon_{\mathrm{BS,RN}}\Psi_{\mathrm{BS,RN}}\left(-\mathrm{T}/\mathrm{K_T}\right)\\ &\quad+\pi\lambda_{\mathrm{BS}}^{(\mathrm{I},2\mathrm{hop})}\Upsilon_{\mathrm{BS,RN}}\Psi_{\mathrm{BS,RN}}\left(-\mathrm{T}\right)\\ B_{\mathrm{RN,MT}}&=\pi\lambda_{\mathrm{BS}}^{(\mathrm{I},2\mathrm{hop})}\Upsilon_{\mathrm{RN,MT}}\Psi_{\mathrm{RN,MT}}\left(-\mathrm{T}\right)\end{aligned}\tag{41}$$

[4]These solutions can be found by using the function FrobeniusSolve of Mathematica. However, for large N_{BS} and N_{RN}^{Tx} memory issues are likely to occur. In such a case, we propose the method described in [49, APPENDIX C].

$$\mathcal{J}_{\mathrm{BS,MT}}\left(\mathrm{T}\right)=\pi\lambda_{\mathrm{BS}}\mathrm{Y}_{\mathrm{BS,MT}}\int_{0}^{\infty}\exp\left(-\pi\lambda_{\mathrm{BS}}\mathrm{Y}_{\mathrm{BS,MT}}\mathrm{y}\right)\exp\left(-\frac{\pi\lambda_{\mathrm{RN}}\mathrm{Y}_{\mathrm{RN,MT}}}{\eta_{\mathrm{cell}}^{2/\beta_{\mathrm{RN,MT}}}}\mathrm{y}^{\frac{\beta_{\mathrm{BS,MT}}}{\beta_{\mathrm{RN,MT}}}}\right)$$
$$\times\sum_{n=0}^{N_{BS}-1}\frac{1}{n!}\left(-\kappa_{0}\mathrm{y}^{\frac{\beta_{\mathrm{BS,MT}}}{2}}\right)^{n}\exp\left(-\frac{\kappa_{0}\mathrm{y}^{\frac{\beta_{\mathrm{BS,MT}}}{2}}\sigma_{N}^{2}\mathrm{T}}{P_{T}/N_{BS}}\right)\sum_{k=0}^{n}\left(\begin{array}{c}n\\k\end{array}\right)\left(-\frac{\sigma_{N}^{2}\mathrm{T}}{P_{T}/N_{BS}}\right)^{n-k}p_{\mathrm{BS,MT}}^{(k)}\left(\mathrm{y}\right)\mathrm{dy},\tag{36}$$

$$\mathcal{J}_{\mathrm{BS,RN}}\left(\mathrm{T}\right)=\pi\lambda_{\mathrm{BS}}\mathrm{Y}_{\mathrm{BS,RN}}\int_{0}^{\infty}\exp\left(-\pi\lambda_{\mathrm{BS}}\mathrm{Y}_{\mathrm{BS,RN}}\mathrm{y}\right)\sum_{n=0}^{N_{BS}-2}\frac{1}{n!}\left(-\kappa_{0}\mathrm{y}^{\frac{\beta_{\mathrm{BS,RN}}}{2}}\right)^{n}\exp\left(-\frac{\kappa_{0}\mathrm{y}^{\frac{\beta_{\mathrm{BS,RN}}}{2}}\sigma_{N}^{2}\mathrm{T}}{P_{T}/N_{BS}}\right)$$
$$\times\sum_{k=0}^{n}\left(\begin{array}{c}n\\k\end{array}\right)\left(-\frac{\sigma_{N}^{2}\mathrm{T}}{P_{T}/N_{BS}}\right)^{n-k}\sum_{m=0}^{k}\left(\begin{array}{c}k\\m\end{array}\right)p_{\mathrm{BS,RN}}^{(m)}\left(\mathrm{y}\right)\left(-\sigma_{\mathrm{SI}}^{2}a_{\mathrm{BS,RN}}\right)^{k-m}$$
$$\times\left(1+\sigma_{\mathrm{SI}}^{2}a_{\mathrm{BS,RN}}\kappa_{0}\mathrm{y}^{\frac{\beta_{\mathrm{BS,RN}}}{2}}\right)^{-1-\kappa+m}(k-m)!\mathrm{dy},\tag{37}$$

$$\mathcal{J}_{\mathrm{RN,MT}}\left(\mathrm{T}\right)=\pi\lambda_{\mathrm{RN}}\mathrm{Y}_{\mathrm{RN,MT}}\int_{0}^{\infty}\exp\left(-\pi\lambda_{\mathrm{RN}}\mathrm{Y}_{\mathrm{RN,MT}}\mathrm{y}\right)\exp\left(-\frac{\pi\lambda_{\mathrm{BS}}\mathrm{Y}_{\mathrm{BS,MT}}}{\eta_{\mathrm{cell}}^{-2/\beta_{\mathrm{BS,MT}}}}\mathrm{y}^{\frac{\beta_{\mathrm{RN,MT}}}{\beta_{\mathrm{BS,MT}}}}\right)$$
$$\times\sum_{n=0}^{N_{RN}^{Tx}-1}\frac{1}{n!}\left(-\kappa_{0}\mathrm{y}^{\frac{\beta_{\mathrm{RN,MT}}}{2}}\right)^{n}\exp\left(-\frac{\kappa_{0}\mathrm{y}^{\frac{\beta_{\mathrm{RN,MT}}}{2}}\sigma_{N}^{2}\mathrm{T}}{P_{T}/N_{RN}^{Tx}}\right)\sum_{k=0}^{n}\left(\begin{array}{c}n\\k\end{array}\right)\left(-\frac{\sigma_{N}^{2}\mathrm{T}}{P_{T}/N_{RN}^{Tx}}\right)^{n-k}p_{\mathrm{RN,MT}}^{(k)}\left(\mathrm{y}\right)\mathrm{dy},\tag{38}$$

and

$$C_{\mathrm{BS,MT}}=\pi\lambda_{\mathrm{BS}}^{(\mathrm{I,2hop})}\Upsilon_{\mathrm{RN,MT}}\Psi_{\mathrm{RN,MT}}\left(-\left(1-K_{T}\right)\frac{N_{BS}}{N_{RN}^{Tx}}\mathrm{T}\right)$$
$$C_{\mathrm{BS,RN}}=\pi\lambda_{\mathrm{BS}}^{(\mathrm{I,2hop})}\frac{2}{\beta_{\mathrm{RN,RN}}}\left(\frac{1-K_{T}}{K_{T}}\frac{N_{BS}}{N_{RN}^{Tx}}\mathrm{T}\right)^{\frac{2}{\beta_{\mathrm{RN,RN}}}}$$
$$\times\Upsilon_{\mathrm{RN,RN}}\Gamma\left(-\frac{2}{\beta_{\mathrm{RN,RN}}}\right)\Gamma\left(\frac{2}{\beta_{\mathrm{RN,RN}}}+1\right)$$
$$C_{\mathrm{RN,MT}}=\pi\lambda_{\mathrm{BS}}^{(\mathrm{I,1hop})}\Upsilon_{\mathrm{BS,MT}}\Psi_{\mathrm{BS,MT}}\left(-\frac{1}{1-K_{T}}\frac{N_{RN}^{Tx}}{N_{BS}}\mathrm{T}\right)$$
$$+\pi\lambda_{\mathrm{BS}}^{(\mathrm{I,2hop})}\Upsilon_{\mathrm{BS,MT}}\Psi_{\mathrm{BS,MT}}\left(-\frac{K_{T}}{1-K_{T}}\frac{N_{RN}^{Tx}}{N_{BS}}\mathrm{T}\right),\tag{42}$$

where

$$\Psi_{\mathrm{X,Y}}\left(x\right)=1-{}_{2}F_{1}\left(1,-\frac{2}{\beta_{\mathrm{X,Y}}};1-\frac{2}{\beta_{\mathrm{X,Y}}};x\right).\tag{43}$$

Proof: See [49, APPENDIX B].

$\mathrm{R}_{\mathrm{xth}}$ is obtained as a solution of the the equation that results by plugging (35) into (23).

Proposition 3. *In the noise-limited region, which can be achieved for sufficiently large N_{BS} and N_{RN}^{Tx}, the coverage probability, which we denote by $\mathrm{P}_{\mathrm{cov}}^{(NL)}\left(\mathrm{T}\right)$, can be approximated as*

$$\mathrm{P}_{\mathrm{cov}}^{(NL)}\left(\mathrm{T}\right)\approx\mathcal{J}_{\mathrm{BS,MT}}^{(NL)}\left(\mathrm{T}\right)+\mathcal{J}_{\mathrm{BS,RN}}^{(NL)}\left(\mathrm{T}\right)\mathcal{J}_{\mathrm{RN,MT}}^{(NL)}\left(\mathrm{T}\right),\tag{44}$$

where $\mathcal{J}_{\mathrm{BS,MT}}^{(NL)}\left(\mathrm{T}\right)$, $\mathcal{J}_{\mathrm{BS,RN}}^{(NL)}\left(\mathrm{T}\right)$, and $\mathcal{J}_{\mathrm{RN,MT}}^{(NL)}\left(\mathrm{T}\right)$ are given by (45)*,* (46)*, and* (45)*, respectively, on the next page.*

Proof: See [49, APPENDIX D].

V. System Model for HD RNs and Comparison

The aim of this section is to present the case of HD RNs and compare the achieved performance with the one of the FD system. Towards this, we consider the same system model as in [38] regarding the phases of communication with HD RNs for which we extend the analysis by considering multiple-antenna BSs and RNs. In particular, the system model consists of two phases that have a duration of one time slot each. In the 1st time slot, only the BSs are allowed to transmit, whereas only the RNs in the 2nd one. Consequently, similar to the analysis for the FD case, and by taking into account that MRT is employed at the BSs and RNs, the instantaneous SINR expressions $\mathrm{SINR}_{\mathrm{BS_0,MT_0}}^{(HD)}$ in the case of a single-hop transmission and $\mathrm{SINR}_{\mathrm{BS_{R0},RN_0}}^{(HD)}$ and $\mathrm{SINR}_{\mathrm{RN_{0)},MT_0}}^{(HD)}$ in the case of a two-hop transmission, are given by

$$\mathrm{SINR}_{\mathrm{BS_0,MT_0}}^{(HD)}=\frac{\left(P_{T}/N_{BS}\right)\left\|\mathbf{h}_{\mathrm{BS_0,MT_0}}\right\|^{2}\mathcal{Z}_{\mathrm{BS_0,MT_0}}^{-1}}{\sigma_{N}^{2}+I_{\mathrm{BS,MT_0}}^{(1)}+I_{\mathrm{BS,MT_0}}^{(2)(HD)}}$$
$$\mathrm{SINR}_{\mathrm{BS_{R0},RN_0}}^{(HD)}=\frac{K_{T}\left(P_{T}/N_{BS}\right)\left\|\mathbf{h}_{\mathrm{BS_{R0},RN_0}}\right\|^{2}\mathcal{Z}_{\mathrm{BS_{R0},RN_0}}^{-1}}{\sigma_{N}^{2}+I_{\mathrm{BS,RN_0}}^{(1)}+I_{\mathrm{BS,RN_0}}^{(2)(HD)}}\tag{48}$$
$$\mathrm{SINR}_{\mathrm{RN_0,MT_0}}^{(HD)}=\frac{\left(1-K_{T}\right)\left(P_{T}/N_{RS}\right)\left\|\mathbf{h}_{\mathrm{RN_0,MT_0}}\right\|^{2}\mathcal{Z}_{\mathrm{RN_0,MT_0}}^{-1}}{\sigma_{N}^{2}+I_{\mathrm{RN,MT_0}}^{(2)(HD)}},$$

where

$$I_{\mathrm{BS,MT_0}}^{(2)(HD)}=\sum_{\mathrm{BS_j}\in\Phi_{\mathrm{BS}}^{(\mathrm{I,2hop})}}K_{T}(P_{T}/N_{BS})\,\mathcal{Z}_{\mathrm{BS_j,MT_0}}^{-1}\left|\mathbf{h}_{\mathrm{BS_j,MT_0}}\mathbf{w}_{\mathrm{BS_j,RN_j}}^{(HD)}\right|^{2}$$
$$\mathbf{1}\left(\mathcal{Z}_{\mathrm{BS_j,MT_0}}>\mathcal{Z}_{\mathrm{BS_0,MT_0}}\right)$$
$$I_{\mathrm{BS,RN_0}}^{(2)(HD)}=\sum_{\mathrm{BS_j}\in\Phi_{\mathrm{BS}}^{(\mathrm{I,2hop})}}K_{T}(P_{T}/N_{BS})\,\mathcal{Z}_{\mathrm{BS_j,RN_0}}^{-1}\left|\mathbf{h}_{\mathrm{BS_j,RN_0}}\mathbf{w}_{\mathrm{BS_j,RN_j}}^{(HD)}\right|^{2}$$
$$\mathbf{1}\left(\mathcal{Z}_{\mathrm{BS_j,RN_0}}>\mathcal{Z}_{\mathrm{BS_{R0},RN_0}}\right)\mathbf{1}\left(\mathcal{Z}_{\mathrm{BS_j,MT_0}}>\eta_{\mathrm{cell}}\mathcal{Z}_{\mathrm{RN_0,MT_0}}\right)$$
$$I_{\mathrm{RN,MT_0}}^{(2)(HD)}=\sum_{\substack{\mathrm{RN}_k\in\Phi_{\mathrm{RN}}^{(\mathrm{I})}\\ \mathrm{card}\left\{\Phi_{\mathrm{RN}}^{(\mathrm{I})}\right\}=\mathrm{card}\left\{\Phi_{\mathrm{BS}}^{(\mathrm{I,2hop})}\right\}}}\left(1-K_{T}\right)\left(P_{T}/N_{RS}\right)\mathcal{Z}_{\mathrm{RN}_k,\mathrm{MT_0}}^{-1}$$
$$\times\left|\mathbf{h}_{\mathrm{RN_k,MT_0}}\mathrm{w}_{\mathrm{RN_k,MT_0}}^{(HD)}\right|^{2}\mathbf{1}\left(\mathcal{Z}_{\mathrm{RN}_k,\mathrm{MT_0}}>\mathcal{Z}_{\mathrm{RN_0,MT_0}}\right).$$

$$\mathcal{J}^{(NL)}_{\mathrm{BS,MT}}\left(\mathrm{T}\right)=\pi\lambda_{\mathrm{BS}}\mathrm{Y}_{\mathrm{BS,MT}}\int_{0}^{\infty}\exp\left(-\pi\lambda_{\mathrm{BS}}\mathrm{Y}_{\mathrm{BS,MT}}\mathrm{y}\right)\exp\left(-\frac{\pi\lambda_{\mathrm{RN}}\mathrm{Y}_{\mathrm{RN,MT}}}{\eta_{\mathrm{cell}}^{2/\beta_{\mathrm{RN,MT}}}}\mathrm{y}^{\frac{\beta_{\mathrm{BS,MT}}}{\beta_{\mathrm{RN,MT}}}}\right)$$
$$\times\exp\left(-\frac{\kappa_0\mathrm{y}^{\frac{\beta_{\mathrm{BS,MT}}}{2}}\sigma_N^2\mathrm{T}}{P_T/N_{BS}}\right)\sum_{n=0}^{N_{BS}-1}\frac{1}{n!}\left(\frac{\kappa_0\mathrm{y}^{\frac{\beta_{\mathrm{BS,MT}}}{2}}\sigma_N^2\mathrm{T}}{P_T/N_{BS}}\right)^{n}\mathrm{dy},\tag{45}$$

$$\mathcal{J}^{(NL)}_{\mathrm{BS,RN}}\left(\mathrm{T}\right)=\pi\lambda_{\mathrm{BS}}\mathrm{Y}_{\mathrm{BS,RN}}\int_{0}^{\infty}\exp\left(-\pi\lambda_{\mathrm{BS}}\mathrm{Y}_{\mathrm{BS,RN}}\mathrm{y}\right)\exp\left(-\frac{\kappa_0\mathrm{y}^{\frac{\beta_{\mathrm{BS,RN}}}{2}}\sigma_N^2\mathrm{T}}{P_T/N_{BS}}\right)\sum_{n=0}^{N_{BS}-2}\frac{1}{n!}\left(-\frac{\kappa_0\mathrm{y}^{\frac{\beta_{\mathrm{BS,RN}}}{2}}\sigma_N^2\mathrm{T}}{P_T/N_{BS}}\right)^{n}\mathrm{dy},\tag{46}$$

$$\mathcal{J}^{(NL)}_{\mathrm{RN,MT}}\left(\mathrm{T}\right)=\pi\lambda_{\mathrm{RN}}\mathrm{Y}_{\mathrm{RN,MT}}\int_{0}^{\infty}\exp\left(-\pi\lambda_{\mathrm{RN}}\mathrm{Y}_{\mathrm{RN,MT}}\mathrm{y}\right)\exp\left(-\frac{\pi\lambda_{\mathrm{BS}}\mathrm{Y}_{\mathrm{BS,MT}}}{\eta_{\mathrm{cell}}^{-2/\beta_{\mathrm{BS,MT}}}}\mathrm{y}^{\frac{\beta_{\mathrm{RN,MT}}}{\beta_{\mathrm{BS,MT}}}}\right)$$
$$\times\exp\left(-\frac{\kappa_0\mathrm{y}^{\frac{\beta_{\mathrm{RN,MT}}}{2}}\sigma_N^2\mathrm{T}}{P_T/N_{RN}^{Tx}}\right)\sum_{n=0}^{N_{RN}^{Tx}-1}\frac{1}{n!}\left(-\frac{\kappa_0\mathrm{y}^{\frac{\beta_{\mathrm{RN,MT}}}{2}}\sigma_N^2\mathrm{T}}{P_T/N_{RN}^{Tx}}\right)^{n}\mathrm{dy},\tag{47}$$

Based on (48), it can be proved with an analysis similar to the FD case that the coverage probability in the HD case, which we denote by $\mathrm{P}_{\mathrm{cov}}^{(HD)}\left(\mathrm{T}\right)$, can be approximated as

$$\mathrm{P}_{\mathrm{cov}}^{(HD)}\left(\mathrm{T}\right)\approx\mathcal{J}^{(HD)}_{\mathrm{BS,MT}}\left(\mathrm{T}\right)+\mathcal{J}^{(HD)}_{\mathrm{BS,RN}}\left(\mathrm{T}\right)\mathcal{J}^{(HD)}_{\mathrm{RN,MT}}\left(\mathrm{T}\right),\tag{49}$$

where $\mathcal{J}^{(HD)}_{\mathrm{BS,MT}}\left(\mathrm{T}\right)$, $\mathcal{J}^{(HD)}_{\mathrm{BS,RN}}\left(\mathrm{T}\right)$, and $\mathcal{J}^{(HD)}_{\mathrm{RN,MT}}\left(\mathrm{T}\right)$ are given by (50), (51), and (52), respectively, on the next page,

$$p^{(k)(HD)}_{\mathrm{X,Y}}\left(\mathrm{y}\right)=\begin{cases}\exp\left(g^{(HD)}_{\mathrm{X,Y}}\left(\mathrm{y}\right)\right),\ k=0\\ \exp\left(g^{(HD)}_{\mathrm{X,Y}}\left(\mathrm{y}\right)\right)\sum\frac{k!}{p_1!...p_k!}\left(\frac{g^{(1)(HD)}_{\mathrm{X,Y}}\left(\mathrm{y}\right)}{1!}\right)^{p_1}\\ \qquad\times...\times\left(\frac{g^{(k)(HD)}_{\mathrm{X,Y}}\left(\mathrm{y}\right)}{k!}\right)^{p_k}\\ \qquad,\ k\geq1,\end{cases}$$

where $\mathrm{X,Y}=\{\left(\mathrm{BS,MT}\right),\left(\mathrm{BS,RN}\right),\left(\mathrm{RN,MT}\right)\}$, $p_1,...p_k$ are given by the non-negative integer solutions of the equation $p_1+2p_2+...kp_k=k$, and

$$g^{(HD)}_{\mathrm{X,Y}}\left(\mathrm{y}\right)=B_{\mathrm{X,Y}}\mathrm{y}$$
$$g^{(k)(HD)}_{\mathrm{BS,MT}}\left(\mathrm{y}\right)=g^{(HD)}_{\mathrm{BS,MT}}\left(\mathrm{y}\right)\prod_{m=1}^{k}\left(\frac{2}{\beta_{\mathrm{BS,MT}}}-\left(m-1\right)\right)\left(\kappa_0\right)^{-m}$$
$$\times\,\mathrm{y}^{-m\frac{\beta_{\mathrm{BS,MT}}}{2}}.\tag{53}$$

By taking into account (49), the xth percentile rate, which we denote by $\mathrm{R}_{\mathrm{xth}}^{(\mathrm{HD})}$, is given by the solution of the following equation:

$$1-\mathcal{J}^{(HD)}_{\mathrm{BS,MT}}\left(2^{\frac{\mathrm{R}_{\mathrm{xth}}^{(\mathrm{HD})}}{\mathrm{B_w}}}-1\right)-\mathcal{J}^{(HD)}_{\mathrm{BS,RN}}\left(2^{\frac{2\mathrm{R}_{\mathrm{xth}}^{(\mathrm{HD})}}{\mathrm{B_w}}}-1\right)$$
$$\times\,\mathcal{J}^{(HD)}_{\mathrm{RN,MT}}\left(2^{\frac{2\mathrm{R}_{\mathrm{xth}}^{(\mathrm{HD})}}{\mathrm{B_w}}}-1\right)=\mathrm{xth}.\tag{54}$$

Proposition 4. *For sufficiently large N_{BS} and N_{RN}^{Tx} (noise-lmited region), the coverage probability in the HD case, which we denote by $\mathrm{P}_{\mathrm{cov}}^{(NL)(HD)}\left(\mathrm{T}\right)$, can be approximated as*

$$\mathrm{P}_{\mathrm{cov}}^{(NL)(HD)}\left(\mathrm{T}\right)\approx\mathcal{J}^{(NL)(HD)}_{\mathrm{BS,MT}}\left(\mathrm{T}\right)+\mathcal{J}^{(NL)(HD)}_{\mathrm{BS,RN}}\left(\mathrm{T}\right)\mathcal{J}^{(NL)(HD)}_{\mathrm{RN,MT}}\left(\mathrm{T}\right),\tag{55}$$

where $\mathcal{J}^{(NL)(HD)}_{\mathrm{BS,MT}}\left(\mathrm{T}\right)$, $\mathcal{J}^{(NL)(HD)}_{\mathrm{BS,RN}}\left(\mathrm{T}\right)$, and $\mathcal{J}^{(NL)(HD)}_{\mathrm{RN,MT}}\left(\mathrm{T}\right)$ are given by (56)*,* (57)*, and* (58)*, respectively, on the next page.*

Proof: (55) can be proved by following the same line of thought as in (44).

Remark 4. *For $\mathcal{B}_{\mathrm{BS}}\neq\infty$, the trends regarding the comparison, in terms of percentile rate, between the network with FD RNs and its HD counterpart depend on whether the networks operate in the interference- or noise-limited region. This depends on the values of N_{BS} and N_{RN}^{Tx}.*

***Interference-limited region**: This is the region of operation if N_{BS} and N_{RN}^{Tx} are not large enough. By comparing* (35) *with* (49)*, we observe that even in the absence of self-interference at RN_0 ($\sigma^2_{\mathrm{SI}}=0$) it holds that $\mathrm{P}_{\mathrm{cov}}\left(\mathrm{T}\right)<\mathrm{P}_{\mathrm{cov}}^{(HD)}\left(\mathrm{T}\right)$. This is due to the fact that $\mathcal{J}_{\mathrm{BS,MT}}\left(\mathrm{T}\right)$, $\mathcal{J}_{\mathrm{BS,RN}}\left(\mathrm{T}\right)$, and $\mathcal{J}_{\mathrm{RN,MT}}\left(\mathrm{T}\right)$ with respect to their counterparts $\mathcal{J}^{(HD)}_{\mathrm{BS,MT}}\left(\mathrm{T}\right)$, $\mathcal{J}^{(HD)}_{\mathrm{BS,RN}}\left(\mathrm{T}\right)$, and $\mathcal{J}^{(HD)}_{\mathrm{RN,MT}}\left(\mathrm{T}\right)$ include the additional terms $C_{\mathrm{BS,MT}}\mathrm{y}^{\frac{\beta_{\mathrm{BS,MT}}}{\beta_{\mathrm{RN,MT}}}}$, $C_{\mathrm{BS,RN}}\mathrm{y}^{\frac{\beta_{\mathrm{BS,RN}}}{\beta_{\mathrm{RN,RN}}}}$, and $C_{\mathrm{RN,MT}}\mathrm{y}^{\frac{\beta_{\mathrm{RN,MT}}}{\beta_{\mathrm{BS,MT}}}}$, respectively. These terms are related to the additional interference terms $i^{(1)}_{\mathrm{RN,MT}_0}$, $i_{\mathrm{RN,RN}_0}$, and $\tilde{i}^{(1)}_{\mathrm{BS,MT}_0}+\tilde{i}^{(2)}_{\mathrm{BS,MT}_0}$, affecting MT_0 during the one-hop communication, RN_0, and MT_0 during the two-hop communication, respectively, in the case of FD RNs compared to the HD RNs case. Hence, due to these terms and the self interference at RN_0 it holds that $\mathcal{J}_{\mathrm{BS,MT}}\left(\mathrm{T}\right)<\mathcal{J}^{(HD)}_{\mathrm{BS,MT}}\left(\mathrm{T}\right)$, $\mathcal{J}_{\mathrm{BS,RN}}\left(\mathrm{T}\right)<\mathcal{J}^{(HD)}_{\mathrm{BS,RN}}\left(\mathrm{T}\right)$, and $\mathcal{J}_{\mathrm{RN,MT}}\left(\mathrm{T}\right)<\mathcal{J}^{(HD)}_{\mathrm{RN,MT}}\left(\mathrm{T}\right)$, which results in $\mathrm{P}_{\mathrm{cov}}\left(\mathrm{T}\right)<\mathrm{P}_{\mathrm{cov}}^{(HD)}\left(\mathrm{T}\right)$.*

Regarding the comparison between $\mathrm{R}_{\mathrm{xth}}$ and $\mathrm{R}_{\mathrm{xth}}^{(HD)}$ in this region, the fact that $\mathrm{P}_{\mathrm{cov}}\left(\mathrm{T}\right)<\mathrm{P}_{\mathrm{cov}}^{(HD)}\left(\mathrm{T}\right)$, whereas the HD network is subject to the HD constraint, means that depending on the values of the path-loss exponents, N_{BS}, N_{RN}^{Tx}, and $\mathcal{B}_{\mathrm{BS}}$,

$$\mathcal{J}_{\mathrm{BS,MT}}^{(HD)}(\mathrm{T}) = \pi\lambda_{\mathrm{BS}}\mathrm{Y}_{\mathrm{BS,MT}}\int_0^{\infty}\exp\left(-\pi\lambda_{\mathrm{BS}}\mathrm{Y}_{\mathrm{BS,MT}}\mathrm{y}\right)\exp\left(-\frac{\pi\lambda_{\mathrm{RN}}\mathrm{Y}_{\mathrm{RN,MT}}}{\eta_{\mathrm{cell}}^{2/\beta_{\mathrm{RN,MT}}}}\mathrm{y}^{\frac{\beta_{\mathrm{BS,MT}}}{\beta_{\mathrm{RN,MT}}}}\right)$$
$$\times\sum_{n=0}^{N_{BS}-1}\frac{1}{n!}\left(-\kappa_0\mathrm{y}^{\frac{\beta_{\mathrm{BS,MT}}}{2}}\right)^n\exp\left(-\frac{\kappa_0\mathrm{y}^{\frac{\beta_{\mathrm{BS,MT}}}{2}}\sigma_N^2\mathrm{T}}{P_T/N_{BS}}\right)\sum_{k=0}^{n}\binom{n}{k}\left(-\frac{\sigma_N^2\mathrm{T}}{P_T/N_{BS}}\right)^{n-k}p_{\mathrm{BS,MT}}^{(k)(HD)}(\mathrm{y})\,\mathrm{dy}. \quad (50)$$

$$\mathcal{J}_{\mathrm{BS,RN}}^{(HD)}(\mathrm{T}) = \pi\lambda_{\mathrm{BS}}\mathrm{Y}_{\mathrm{BS,RN}}\int_0^{\infty}\exp\left(-\pi\lambda_{\mathrm{BS}}\mathrm{Y}_{\mathrm{BS,RN}}\mathrm{y}\right)\sum_{n=0}^{N_{BS}-1}\frac{1}{n!}\left(-\kappa_0\mathrm{y}^{\frac{\beta_{\mathrm{BS,RN}}}{2}}\right)^n\exp\left(-\frac{\kappa_0\mathrm{y}^{\frac{\beta_{\mathrm{BS,RN}}}{2}}\sigma_N^2\mathrm{T}}{P_T/N_{BS}}\right)$$
$$\times\sum_{k=0}^{n}\binom{n}{k}\left(-\frac{\sigma_N^2\mathrm{T}}{P_T/N_{BS}}\right)^{n-k}p_{\mathrm{BS,RN}}^{(k)(HD)}(\mathrm{y})\,\mathrm{dy}. \quad (51)$$

$$\mathcal{J}_{\mathrm{RN,MT}}^{(HD)}(\mathrm{T}) = \pi\lambda_{\mathrm{RN}}\mathrm{Y}_{\mathrm{RN,MT}}\int_0^{\infty}\exp\left(-\pi\lambda_{\mathrm{RN}}\mathrm{Y}_{\mathrm{RN,MT}}\mathrm{y}\right)\exp\left(-\frac{\pi\lambda_{\mathrm{BS}}\mathrm{Y}_{\mathrm{BS,MT}}}{\eta_{\mathrm{cell}}^{-2/\beta_{\mathrm{BS,MT}}}}\mathrm{y}^{\frac{\beta_{\mathrm{RN,MT}}}{\beta_{\mathrm{BS,MT}}}}\right)$$
$$\times\sum_{n=0}^{N_{RN}^{Tx}-1}\frac{1}{n!}\left(-\kappa_0\mathrm{y}^{\frac{\beta_{\mathrm{RN,MT}}}{2}}\right)^n\exp\left(-\frac{\kappa_0\mathrm{y}^{\frac{\beta_{\mathrm{RN,MT}}}{2}}\sigma_N^2\mathrm{T}}{P_T/N_{RN}^{Tx}}\right)\sum_{k=0}^{n}\binom{n}{k}\left(-\frac{\sigma_N^2\mathrm{T}}{P_T/N_{RN}^{Tx}}\right)^{n-k}p_{\mathrm{RN,MT}}^{(k)(HD)}(\mathrm{y})\,\mathrm{dy}, \quad (52)$$

$$\mathcal{J}_{\mathrm{BS,MT}}^{(NL)(HD)}(\mathrm{T}) = \pi\lambda_{\mathrm{BS}}\mathrm{Y}_{\mathrm{BS,MT}}\int_0^{\infty}\exp\left(-\pi\lambda_{\mathrm{BS}}\mathrm{Y}_{\mathrm{BS,MT}}\mathrm{y}\right)\exp\left(-\frac{\pi\lambda_{\mathrm{RN}}\mathrm{Y}_{\mathrm{RN,MT}}}{\eta_{\mathrm{cell}}^{2/\beta_{\mathrm{RN,MT}}}}\mathrm{y}^{\frac{\beta_{\mathrm{BS,MT}}}{\beta_{\mathrm{RN,MT}}}}\right)$$
$$\times\exp\left(-\frac{\kappa_0\mathrm{y}^{\frac{\beta_{\mathrm{BS,MT}}}{2}}\sigma_N^2\mathrm{T}}{P_T/N_{BS}}\right)\sum_{n=0}^{N_{BS}-1}\frac{1}{n!}\left(\frac{\kappa_0\mathrm{y}^{\frac{\beta_{\mathrm{BS,MT}}}{2}}\sigma_N^2\mathrm{T}}{P_T/N_{BS}}\right)^n\mathrm{dy}, \quad (56)$$

$$\mathcal{J}_{\mathrm{BS,RN}}^{(NL)(HD)}(\mathrm{T}) = \pi\lambda_{\mathrm{BS}}\mathrm{Y}_{\mathrm{BS,RN}}\int_0^{\infty}\exp\left(-\pi\lambda_{\mathrm{BS}}\mathrm{Y}_{\mathrm{BS,RN}}\mathrm{y}\right)\exp\left(-\frac{\kappa_0\mathrm{y}^{\frac{\beta_{\mathrm{BS,RN}}}{2}}\sigma_N^2\mathrm{T}}{P_T/N_{BS}}\right)\sum_{n=0}^{N_{BS}-1}\frac{1}{n!}\left(-\frac{\kappa_0\mathrm{y}^{\frac{\beta_{\mathrm{BS,RN}}}{2}}\sigma_N^2\mathrm{T}}{P_T/N_{BS}}\right)^n\mathrm{dy}, \quad (57)$$

$$\mathcal{J}_{\mathrm{RN,MT}}^{(NL)(HD)}(\mathrm{T}) = \pi\lambda_{\mathrm{RN}}\mathrm{Y}_{\mathrm{RN,MT}}\int_0^{\infty}\exp\left(-\pi\lambda_{\mathrm{RN}}\mathrm{Y}_{\mathrm{RN,MT}}\mathrm{y}\right)\exp\left(-\frac{\pi\lambda_{\mathrm{BS}}\mathrm{Y}_{\mathrm{BS,MT}}}{\eta_{\mathrm{cell}}^{-2/\beta_{\mathrm{BS,MT}}}}\mathrm{y}^{\frac{\beta_{\mathrm{RN,MT}}}{\beta_{\mathrm{BS,MT}}}}\right)$$
$$\times\exp\left(-\frac{\kappa_0\mathrm{y}^{\frac{\beta_{\mathrm{RN,MT}}}{2}}\sigma_N^2\mathrm{T}}{P_T/N_{RN}^{Tx}}\right)\sum_{n=0}^{N_{RN}^{Tx}-1}\frac{1}{n!}\left(-\frac{\kappa_0\mathrm{y}^{\frac{\beta_{\mathrm{RN,MT}}}{2}}\sigma_N^2\mathrm{T}}{P_T/N_{RN}^{Tx}}\right)^n\mathrm{dy}, \quad (58)$$

R_{xth} can be larger or smaller than $\mathrm{R}_{\mathrm{xth}}^{(HD)}$. In particular, it is expected that $\mathrm{R}_{\mathrm{xth}} < \mathrm{R}_{\mathrm{xth}}^{(HD)}$ for $\sigma_{\mathrm{SI}}^2 \neq 0$ and small N_{BS}, N_{RN}^{Tx}, and $\beta_{\mathrm{RN,RN}}$ (which means that the interference that RN_0 experiences due to the transmissions of the interfering relays is strong). However, as N_{BS} and N_{RN}^{Tx} increase a crossing point is expected above which $\mathrm{R}_{\mathrm{xth}} > \mathrm{R}_{\mathrm{xth}}^{(HD)}$ holds.

***Noise-limited region**: This is the region of operation if N_{BS} and N_{RN}^{Tx} are sufficiently large. In this region it holds that $\mathrm{P}_{\mathrm{cov}}^{(NL)}(\mathrm{T}) \approx \mathrm{P}_{\mathrm{cov}}^{(NL)(HD)}(\mathrm{T})$, which is due to the fact that $\mathcal{J}_{\mathrm{BS,MT}}^{(NL)}(\mathrm{T}) = \mathcal{J}_{\mathrm{BS,MT}}^{(NL)(HD)}(\mathrm{T})$, $\mathcal{J}_{\mathrm{BS,RN}}^{(NL)}(\mathrm{T}) \approx \mathcal{J}_{\mathrm{BS,RN}}^{(NL)(HD)}(\mathrm{T})$, and $\mathcal{J}_{\mathrm{RN,MT}}^{(NL)}(\mathrm{T}) = \mathcal{J}_{\mathrm{RN,MT}}^{(NL)(HD)}(\mathrm{T})$ from what we can observe by comparing* (45)*,* (46)*, and* (47) *with* (56)*,* (57)*, and* (58)*, respectively. Consequently, due to the HD constraint it holds that $\mathrm{R}_{\mathrm{xth}}^{'} > \mathrm{R}_{\mathrm{xth}}^{'(HD)}$.*

VI. Applicability and Limitations of the Derived Expressions

The aim of this section is to provide a discussion on the main assumptions that lead to the derived analytical expressions of the percentile rate and whether these assumptions limit their applicability.

The first main assumption is that we model the position and number of BSs and RNs as 2 independent PPPs. This would mean that the placement of RNs does not depend on the placement of BSs. In reality, it is not expected of course that, in terms of performance, placing the RNs independently of the position of the BSs is the optimal approach. What is expected as a real implementation is that the position of the RNs is optimized with respect to some performance maximization criteria, conditioned on the position of the BSs. However,

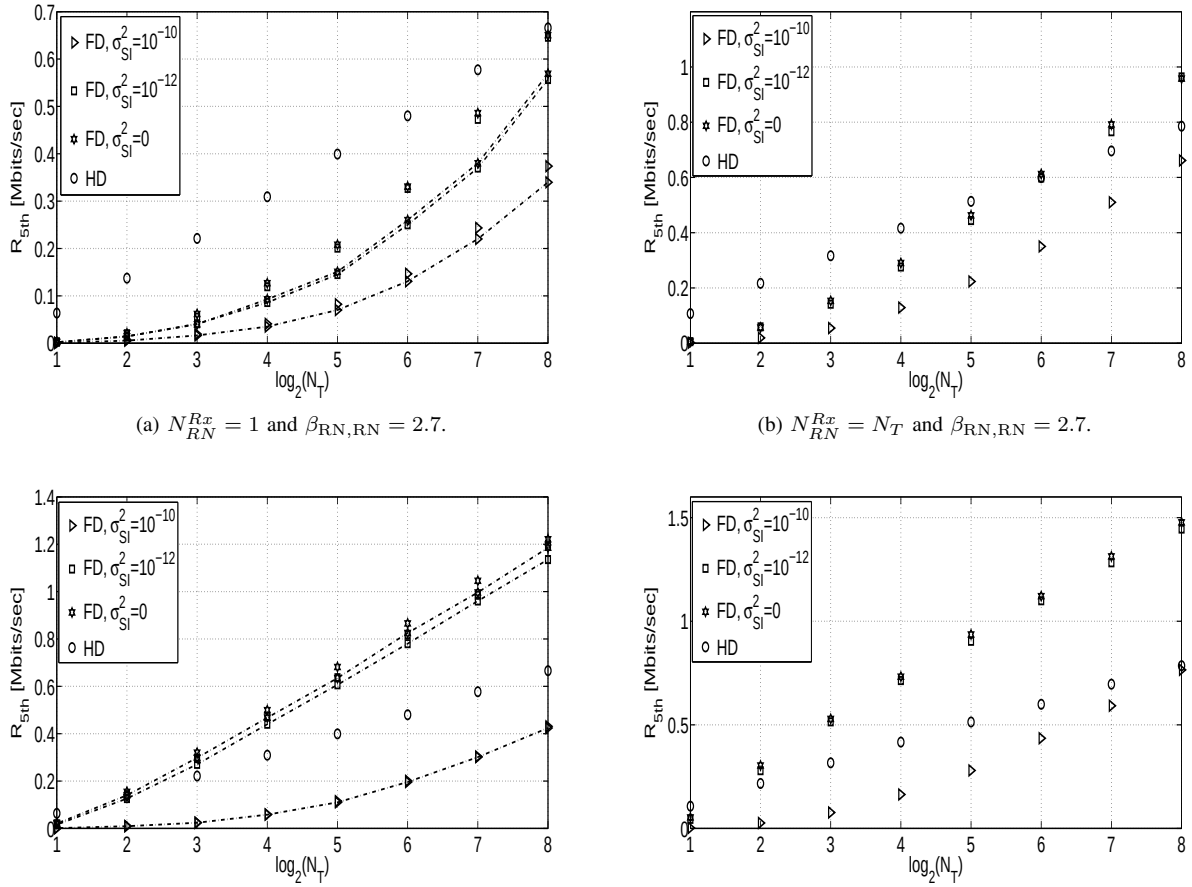

(a) $N_{RN}^{Rx} = 1$ and $\beta_{\mathrm{RN,RN}} = 2.7$.

(b) $N_{RN}^{Rx} = N_T$ and $\beta_{\mathrm{RN,RN}} = 2.7$.

(c) $N_{RN}^{Rx} = 1$ and $\beta_{\mathrm{RN,RN}} = 3.3$.

(d) $N_{RN}^{Rx} = N_T$ and $\beta_{\mathrm{RN,RN}} = 3.3$.

Fig. 2: $\mathrm{R_{5th}}$ vs. $log_2\left(N_T\right)$ for $\beta_{\mathrm{BS,MT}} = 4$, $\beta_{\mathrm{BS,RN}} = \beta_{\mathrm{RN,MT}} = 3$, and $\mathcal{B}_{\mathrm{BS}} = 1$. Dotted lines with markers illustrate the analytical model, whereas markers illustrate Monte Carlo simulations.

we are confident that the observed trends (which the main purpose of our work), such as the behavior as the number of antennas increases, cannot be affected by such a case. Secondly, another important assumption is that we do not consider pilot contamination and we also assume that there is a perfect CSI. Regarding pilot contamination, as we mention in the manuscript it can be eliminated based on the method of [42], for instance. In the case that it cannot be eliminated, according to [41, Eq. (20)] for a massive (practically very large) number of antennas pilot contamination results in a term at the denominator of the SINR expressions that depends on the shadowing and pathloss of the interfering nodes towards the node of interest. If the number of antennas is not massive, still such a term would appear at the denominator of the SINR expressions, but it would depend also on the channel fading coefficients from each of the antennas of the interfering nodes towards the node of interest. In any case, regardless of whether there is a massive or moderate number of antennas at the node of interest and the interfering nodes, the same term in the denominator of the SINR expressions at RN_0 and MT_0 would appear for the cases with FD and HD RNs and also at MT_0 for the baseline network without RNs. As a result, the observed trends would not be affected.

As far as perfect CSI is concerned, in slowly-changing channels (low mobility) such an acquisition can be feasible. However, even if this assumption seems unrealistic, imperfect channel estimates would not also affect the observed trends regarding the comparison of the FD case with the HD one and the case without RNs since all of the cases would be affected in the same way. Let alone that for a massive number of antennas the effect of imperfect channel estimates is eliminated, as it is proved in [41].

All in all, the bottom line from the above discussion is that the aim of our work is the comparative study of the FD RNs case with its HD counterpart and the network without RNs. As we justified above, the trends from this comparison, which is our goal, cannot be affected by including the above real-world considerations.

VII. Numerical Results

Our aim in this section is twofold: i) To validate Remark 4 regarding the comparison of the FD with HD case. ii) To examine whether the inclusion of the FD RNs enhances the performance of the no-RNs network and whether a moderate or a high antenna number is sufficient to achieve this if it is the case.

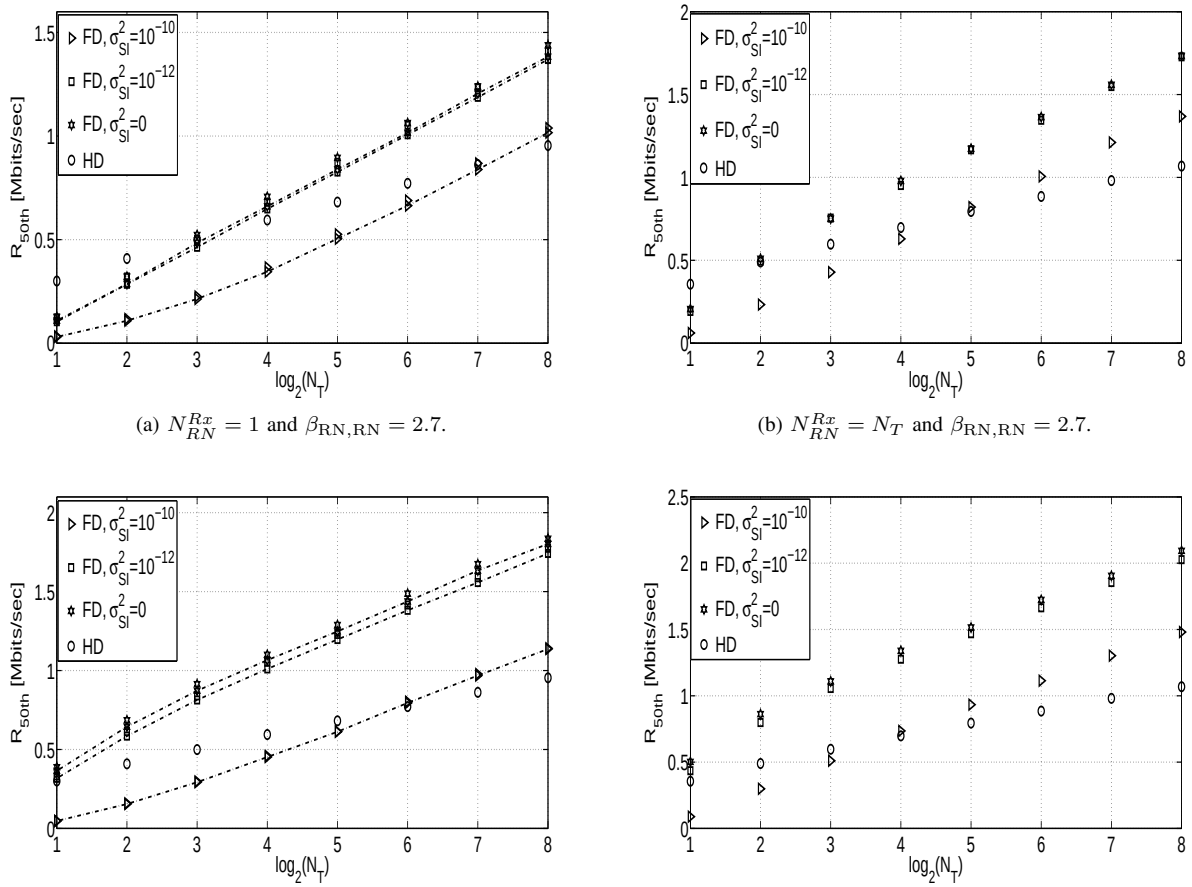

(a) $N_{RN}^{Rx} = 1$ and $\beta_{\mathrm{RN,RN}} = 2.7$.

(b) $N_{RN}^{Rx} = N_T$ and $\beta_{\mathrm{RN,RN}} = 2.7$.

(c) $N_{RN}^{Rx} = 1$ and $\beta_{\mathrm{RN,RN}} = 3.3$.

(d) $N_{RN}^{Rx} = N_T$ and $\beta_{\mathrm{RN,RN}} = 3.3$.

Fig. 3: $\mathrm{R}_{50\mathrm{th}}$ vs. $log_2\left(N_T\right)$ for $\beta_{\mathrm{BS,MT}} = 4$, $\beta_{\mathrm{BS,RN}} = \beta_{\mathrm{RN,MT}} = 3$, and $\mathcal{B}_{\mathrm{BS}} = 1$. Dotted lines with markers illustrate the analytical model, whereas markers illustrate Monte Carlo simulations.

Regarding the simulation parameters, we consider $P_T = 45$ dBm, $K_T = 0.5$, $N_{BS} = N_{RN}^{Tx} = N_T$, $\mathcal{F}_{\mathrm{dB}} = 10$ dB, $f_c = 2$ GHz is the carrier frequency, $\mu_{X,Y} = 0$ dB, $\sigma_{X,Y} = 4$ dB, $\mathrm{B_W} = 180$ kHz, which is the transmission bandwidth of a resource block in the LTE-A standard, $\delta = 50$, $k_{\mathrm{MT}} = 10$, $\lambda_{\mathrm{BS}} = 1/\left(\pi R_{\mathrm{cell}}^2\right)$, where $R_{\mathrm{cell}} = 200$ m is the average radius of a cell, and $\lambda_{\mathrm{RN}} = 3\lambda_{\mathrm{BS}}$. Regarding the Monte Carlo simulations, the same principles as in [38, Section V] apply. In addition, the simulations refer to the exact network setup without considering the SINR approximations of Section IV-B.

In addition, as far as the path-loss exponents $\beta_{\mathrm{BS,MT}}$, $\beta_{\mathrm{BS,RN}}$, $\beta_{\mathrm{RN,MT}}$, and $\beta_{\mathrm{RN,RN}}$ are concerned, we consider scenarios where $\beta_{\mathrm{BS,MT}} > \beta_{\mathrm{BS,RN}}, \beta_{\mathrm{RN,MT}}, \beta_{\mathrm{RN,RN}}$. The intuition behind this lies on the fact that in realistic scenarios RNs are expected to be needed to assist the communication between BSs and MTs for high $\beta_{\mathrm{BS,MT}}$. Considering this, RNs are expected to be deployed in a way that the BS-RN and RN-MT links are stronger than the BS-MT links, which means that RNs are likely to be deployed on rooftops [50]. This would likely also make $\beta_{\mathrm{RN,RN}}$ smaller than $\beta_{\mathrm{BS,MT}}$.

Regarding Remark 4, for $\beta_{\mathrm{BS,MT}} = 4$, $\beta_{\mathrm{BS,RN}} = \beta_{\mathrm{RN,MT}} = 3$, and $\mathcal{B}_{\mathrm{BS}} = 1$, Figs. 2 and 3 illustrate $\mathrm{R}_{5\mathrm{th}}$ and $\mathrm{R}_{50\mathrm{th}}$ vs. $\log_2\left(N_T\right)$, respectively, for the FD and HD cases, N_{RN}^{Rx} equal to 1 and N_T, two values of $\beta_{\mathrm{RN,RN}}$, and different values of σ_{SI}^2 in the FD case[5]. As we observe from Fig. 2 (a) and (c) that correspond to the case $N_{RN}^{Rx} = 1$, for which we have derived the analytical framework, there is only a small gap between the analytical model and the simulations. In addition, for $\beta_{\mathrm{RN,RN}} = 2.7$ we see that $\mathrm{R}_{5\mathrm{th}}$ for the HD case is higher than the corresponding one for the FD case even under the absence of self interference if N_T is not sufficiently high. Moreover, we observe that a value of σ_{SI}^2 equal to 10^{-12} is required so that a performance almost the same as the one without self interference is achieved. On the other hand, a value of σ_{SI}^2 equal to 10^{-10} results in a substantial performance degradation. This is a clear indication that ways to significantly mitigate σ_{SI}^2 need to be devised, such as placing the RNs in sites which result in such small σ_{SI}^2 values according to the particular topology of buildings and obstacles in the area of deployment. Finally, by comparing the plots for $N_{RN}^{Rx} = 1$ with the ones for $N_{RN}^{Rx} = N_T$ we observe that in the latter case the crossing point over which the FD network outperforms the HD one occurs for a lower N_T. This is due to the higher on average $\mathrm{SINR}_{\mathrm{BS_{R0},RN_0}}$ since

[5] $\mathrm{R}_{5\mathrm{th}}$ and $\mathrm{R}_{50\mathrm{th}}$ correspond to the rates of cell-edge and cell-median MTs, respectively [51].

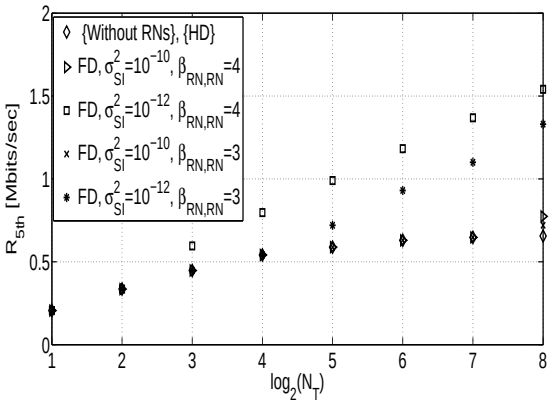

(a) $\mathrm{R}_{5\mathrm{th}}$

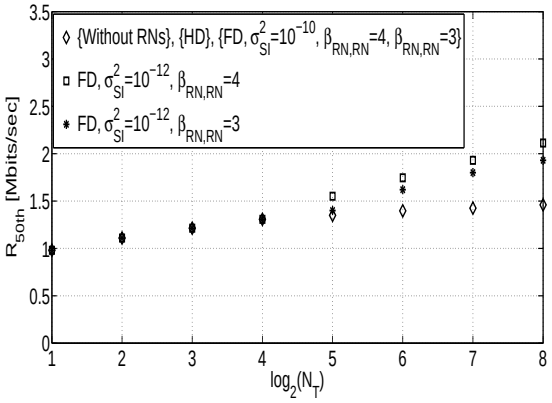

(b) $\mathrm{R}_{50\mathrm{th}}$

Fig. 4: Simulation results of the optimal values of $\mathrm{R}_{5\mathrm{th}}$ and $\mathrm{R}_{50\mathrm{th}}$ ($\mathcal{B}_{\mathrm{BS}}$ that maximizes them) vs. $\log_2(N_T)$ for $\beta_{\mathrm{BS,MT}} = 4.5$, $\beta_{\mathrm{BS,RN}} = \beta_{\mathrm{RN,MT}} = 3$, and $R_{RN}^{Rx} = N_T$.

multiple antennas are used for reception and combining at RN_0. Finally, for the higher value of $\beta_{\mathrm{RN,RN}} = 3.3$, which means that the interference that RN_0 experiences due to other RN transmissions is smaller than the $\beta_{\mathrm{RN,RN}} = 2.7$ case, we observe from Fig. 2 (c) and (d) that for the $\sigma_{\mathrm{SI}}^2 = 10^{-12}$ and $\sigma_{\mathrm{SI}}^2 = 0$ cases the FD network significantly outperforms the HD one, which is in contrast to the $\beta_{\mathrm{RN,RN}} = 2.7$ case. This is another indication that the placement of RNs should be performed in a way that $\beta_{\mathrm{RN,RN}}$ is as large as possible, apart from the fact that σ_{SI}^2 should be as small as possible. All the above trends validate the expected ones from the analytical model according to Remark 4.

As far as $R_{50\mathrm{th}}$ is concerned, from Fig. 3 we observe the same trends for increasing N_T as with $R_{5\mathrm{th}}$ except for the fact that now for $\sigma_{\mathrm{SI}}^2 = 10^{-12}$ and $\sigma_{\mathrm{SI}}^2 = 0$ the network with FD RNs outperforms its HD counterpart even for low and moderate N_T when $\beta_{\mathrm{RN,RN}} = 2.7$. This is justified by the smaller network interference due to the larger distances from their associated cells that the cell-median MTs experience compared to the cell-edge ones. This means that a smaller number of antennas is required to sufficiently mitigate it. Due to the smaller network interference, we also observe that for relatively high N_T even when $\sigma_{\mathrm{SI}}^2 = 10^{-10}$ the FD network can outperform the HD one.

Now, regarding the possible rate gains when FD RNs are deployed compared to no-RNs case, in Fig. 4 we illustrate $R_{5\mathrm{th}}$ and $\mathrm{R}_{50\mathrm{th}}$ vs. $\log_2(N_T)$ for the FD and no-RNs ($\mathcal{B}_{\mathrm{BS}} = \infty$) cases with parameters $\beta_{\mathrm{BS,MT}} = 4.5$, $\beta_{\mathrm{BS,RN}} = \beta_{\mathrm{RN,MT}} = 3$, and $N_{RN}^{Rx} = N_T$. For the FD case, the values of $\mathcal{B}_{\mathrm{BS}}$ used for $R_{5\mathrm{th}}$ and $R_{50\mathrm{th}}$ are the ones that maximize them, respectively, which were obtained through a linear search. For reasons of comparison, we also present the corresponding values of $\mathrm{R}_{5\mathrm{th}}^{(HD)}$ and $\mathrm{R}_{50\mathrm{th}}^{(HD)}$ for the HD case in which again we consider the corresponding values of $\mathcal{B}_{\mathrm{BS}}$ that maximize them, respectively. What we can observe from Fig. 4 are the following: i) The HD and no-RNs cases overlap regardless of the N_T value, which means that HD relaying-cellular networks cannot outperform the ones without RNs in terms of rate, which is reasonable due to their HD constraint. ii) FD networks can outperform the ones without RNs in terms of both $R_{5\mathrm{th}}$ and $\mathrm{R}_{50\mathrm{th}}$ when N_T is sufficiently high and σ_{SI}^2 adequately small. In particular, the value 10^{-12} gives a performance almost the same as with the no self-interference case. ii) The rate gains of cell-edge MTs ($\mathrm{R}_{5\mathrm{th}}$) with respect to the no-RNs case are higher than the ones of the cell-median MTs ($\mathrm{R}_{50\mathrm{th}}$). This is justified by the higher network interference that the former MTs experience compared to the latter ones, as aforementioned, which makes the increase in N_T more beneficial for those MTs as far as interference mitigation is concerned.

VIII. Conclusions

Our aim in this work has been to investigate, from a system-level point of view, whether the deployment of multiple-antenna FD RNs can enhance the rate of a typical cellular network with multiple-antenna BSs operating in the downlink. By considering a system-level abstraction modeling based on the widely used tool of stochastic geometry, for the special case of one receive antenna at the RNs we have derived an analytical expression for the xth percentile rate. The analysis exhibits a relatively close match with the simulation results and reveals the following trends, which are validated by means of Monte Carlo simulations: i) A network with HD RNs can outperform its FD counterpart, in terms of achievable rate, even in the absence of self-interference at the RNs if the number of antennas at the BSs and RNs is not sufficiently large. This is in contrast to the outcomes of literature works that do not consider the effect of network interference. ii) Even if the HD network substantially outperforms the one with FD RNs for a particular number of antennas, increasing the antennas results in a crossing point over which the FD network becomes better in terms of performance.

Furthermore, the simulation results show that important rate gains compared to the no-RNs case can be achieved for both cell-edge and cell-median MTs as the number of antennas at the BSs and FD RNs increases and for a substantially small variance of the self interference. This poses significant challenges regarding the design and placement of the FD RNs. In contrast, no rate gains, regardless of the number of antennas, can be achieved when the RNs follow the HD principle, which is due to the HD constraint.

To the best of our knowledge, such a study is the first system-level study regarding the potential of FD-based relaying and, in our opinion, the promising outcomes constitute a guideline for the system designers of next-generation relay-based cellular networks. The fact though that a large number of antennas is required to achieve the benefits of FD relaying if the self-interference level is not small enough crates issues regarding the available space at the BSs and RNs to accommodate this number of antennas. This motivates us to study such a network in a millimeter-wave setup as future work due to the significantly smaller wavelength, which enables the packing of the same number of antennas inside a smaller space.

ACKNOWLEDGMENTS

The authors would like to cordially thank the editor and anonymous reviewers whose thorough comments and suggestions have substantially improved this manuscript.

APPENDIX

Proof of Lemma 1

For $N_{RN}^{Rx} = 1$, it holds that $\mathbf{u}_{\mathrm{BS_{R0}},\mathrm{RN_0}}^{(l)} = 1$ and $\mathbf{u}_{\mathrm{BS_{R0}},\mathrm{RN_0}}^{(r)} = \frac{\mathbf{h}_{\mathrm{BS_{R0}},\mathrm{RN_0}}^{H}}{\left\|\mathbf{h}_{\mathrm{BS_{R0}},\mathrm{RN_0}}\right\|}$, where $\mathbf{h}_{\mathrm{BS_{R0}},\mathrm{RN_0}} \in \mathbb{CN}^{1\times(N_{BS})}$ is the channel vector that corresponds to the $\mathrm{BS_{R0}} - \mathrm{RN_0}$ link. Consequently, it holds that

$$\begin{aligned}
&\left|\mathbf{w}_{\mathrm{BS_{R0}RN_0}}^{Rx}\mathbf{H}_{\mathrm{BS_{R0}RN_0}}\mathbf{w}_{\mathrm{BS_{R0}RN_0}}^{Tx}\right|^2 = \left\|\mathbf{P}_{\mathbf{h}_{\mathrm{BS_{R0}},\mathrm{MT_0}}}\mathbf{h}_{\mathrm{BS_{R0},RN_0}}^{H}\right\|^2 \\
&= \mathbf{h}_{\mathrm{BS_{R0}},\mathrm{RN_0}}\mathbf{U}\left(\mathbf{I}_{N_{BS}} - \mathrm{diag}\left\{1,0,\cdots,0\right\}\right)\mathbf{U}^{H}\mathbf{h}_{\mathrm{BS_{R0}},\mathrm{RN_0}}^{H} \\
&= \left\|\tilde{\mathbf{h}}_{\mathrm{BS_{R0}},\mathrm{RN_0}}\right\|^2, \qquad (59)
\end{aligned}$$

where $\mathbf{U}$ is a unitary matrix, $\hat{\mathbf{h}}_{\mathrm{BS_{R0}},\mathrm{RN_0}} = \mathbf{h}_{\mathrm{BS_{R0}},\mathrm{RN_0}}\mathbf{U}$, and $\tilde{\mathbf{h}}_{\mathrm{BS_{R0}},\mathrm{RN_0}} \in \mathbb{CN}^{1\times(N_{BS}-1)}$.

REFERENCES

[1] M. O. Hasna and M. S. Alouini, "End-to-end performance of transmission systems with relays over rayleigh-fading channels," *IEEE Trans. Wireless Commun.*, vol. 2, no. 6, pp. 1126–1131, Nov. 2003.

[2] G. K. Karagiannidis, T. A. Tsiftsis, and R. K. Mallik, "Bounds for multihop relayed communications in nakagami-m fading," *IEEE Trans. Commun.*, vol. 54, no. 1, pp. 18–22, Jan. 2006.

[3] S. Ikki and M. H. Ahmed, "Performance analysis of cooperative diversity wireless networks over nakagami-m fading channel," *IEEE Commun. Lett.*, vol. 11, no. 4, pp. 334–336, Apr. 2007.

[4] M. D. Renzo, F. Graziosi, and F. Santucci, "A unified framework for performance analysis of csi-assisted cooperative communications over fading channels," *IEEE Trans. Commun.*, vol. 57, no. 9, pp. 2551–2557, Sep. 2009.

[5] N. C. Beaulieu and S. S. Soliman, "Exact analysis of multihop amplify-and-forward relaying systems over general fading links," *IEEE Trans. Commun.*, vol. 60, no. 8, pp. 2123–2134, Aug. 2012.

[6] H. A. Suraweera, H. K. Garg, and A. Nallanathan, "Performance analysis of two hop amplify-and-forward systems with interference at the relay," *IEEE Commun. Lett.*, vol. 14, no. 8, pp. 692–694, Aug. 2010.

[7] F. S. Al-Qahtani, T. Q. Duong, C. Zhong, K. A. Qaraqe, and H. Alnuweiri, "Performance analysis of dual-hop af systems with interference in nakagami- m fading channels," *IEEE Signal Process. Lett.*, vol. 18, no. 8, pp. 454–457, Aug. 2011.

[8] C. Zhong, H. A. Suraweera, A. Huang, Z. Zhang, and C. Yuen, "Outage probability of dual-hop multiple antenna af relaying systems with interference," *IEEE Trans. Commun.*, vol. 61, no. 1, pp. 108–119, Jan. 2013.

[9] S. Hong, J. Brand, J. I. Choi, M. Jain, J. Mehlman, S. Katti, and P. Levis, "Applications of self-interference cancellation in 5g and beyond," *IEEE Commun. Mag.*, vol. 52, no. 2, pp. 114–121, Feb. 2014.

[10] T. Riihonen, S. Werner, and R. Wichman, "Mitigation of loopback self-interference in full-duplex mimo relays," *IEEE Signal Process. Lett.*, vol. 59, no. 12, pp. 5983–5993, Dec. 2011.

[11] T. Kwon, S. Lim, S. Choi, and D. Hong, "Optimal duplex mode for df relay in terms of the outage probability," *IEEE Trans. Veh. Technol.*, vol. 59, no. 7, pp. 3628–3634, Sep. 2010.

[12] G. Liu, F. R. Yu, H. Ji, V. C. M. Leung, and X. Li, "In-band full-duplex relaying: A survey, research issues and challenges," *IEEE Commun. Surveys Tuts.*, vol. 17, no. 2, pp. 500–524, 2nd Quart. 2015.

[13] "Multi-hop relay system evaluation methodology," IEEE 802.16 Relay Task Group, Tech. Rep., Feb. 2007.

[14] T. Yu, S. H. Han, S. Jung, J. Son, Y. Chang, and H. Kang, "Proposal for full duplex relay," IEEE 802.16 Broadband Wireless Access Working Group, Tech. Rep., May 2008.

[15] S. W. Peters, A. Y. Panah, K. T. Truong, and R. W. Heath, "Relay architectures for 3gpp lte-advanced," *EURASIP Journal on Wireless Communications and Networking*, vol. 2009, no. 1, p. 618787, 2009. [Online]. Available: http://dx.doi.org/10.1155/2009/618787

[16] "Text proposal on inband full duplex relay for tr 36.814," 3GPP TSG RAN WG1 R1-101659, Tech. Rep., Feb. 2010.

[17] L. J. Rodríguez, N. H. Tran, and T. Le-Ngoc, "Performance of full-duplex af relaying in the presence of residual self-interference," *IEEE J. Sel. Areas Commun.*, vol. 32, no. 9, pp. 1752–1764, Sep. 2014.

[18] T. Riihonen, S. Werner, R. Wichman, and E. Z. B., "On the feasibility of full-duplex relaying in the presence of loop interference," in *Proc. 10th IEEE Workshop Signal Process. Adv. Wireless Commun.*, June 2009, pp. 275–279.

[19] M. Mohammadi, H. A. Suraweera, Y. Cao, I. Krikidis, and C. Tellambura, "Full-duplex radio for uplink/downlink wireless access with spatially random nodes," *IEEE Trans. Commun.*, vol. 63, no. 12, pp. 5250–5266, Dec. 2015.

[20] H. Q. Ngo, H. A. Suraweera, M. Matthaiou, and E. G. Larsson, "Multipair full-duplex relaying with massive arrays and linear processing," *IEEE J. Sel. Areas Commun.*, vol. 32, no. 9, pp. 1721–1737, Sep. 2014.

[21] H. A. Suraweera, I. Krikidis, G. Zheng, C. Yuen, and P. J. Smith, "Low-complexity end-to-end performance optimization in mimo full-duplex relay systems," *IEEE Trans. Wireless Commun.*, vol. 13, no. 2, pp. 913–927, Feb. 2014.

[22] A. Ghosh, N. Mangalvedhe, R. Ratasuk, B. Mondal, M. Cudak, E. Visotsky, T. A. Thomas, J. G. Andrews, P. Xia, H. S. Jo, H. S. Dhillon, and T. D. Novlan, "Heterogeneous cellular networks: From theory to practice," *IEEE Commun. Mag.*, vol. 50, no. 6, pp. 54–64, June 2012.

[23] S. Goyal, P. Liu, S. S. Panwar, R. A. Difazio, R. Yang, and E. Bala, "Full duplex cellular systems: will doubling interference prevent doubling capacity?" *IEEE Commun. Mag.*, vol. 53, no. 5, pp. 121–127, May 2015.

[24] J. G. Andrews, F. Baccelli, and R. K. Ganti, "A tractable approach to coverage and rate in cellular networks," *IEEE Trans. Commun.*, vol. 59, no. 11, pp. 3122–3134, Nov. 2011.

[25] A. Guo and M. Haenggi, "Spatial stochastic models and metrics for the structure of base stations in cellular networks," *IEEE Trans. Wireless Commun.*, vol. 12, no. 11, pp. 5800–5812, Nov. 2013.

[26] H. S. Dhillon, M. Kountouris, and J. G. Andrews, "Downlink mimo hetnets: Modeling, ordering results and performance analysis," *IEEE Trans. Wireless Commun.*, vol. 12, no. 10, pp. 5208–5222, Oct. 2013.

[27] M. D. Renzo and W. Lu, "Stochastic geometry modeling and performance evaluation of mimo cellular networks using the equivalent-in-distribution (eid)-based approach," *IEEE Trans. Commun.*, vol. 63, no. 3, pp. 977–996, Mar. 2015.

[28] H. S. Dhillon, R. K. Ganti, F. Baccelli, and J. G. Andrews, "Modeling and analysis of k-tier downlink heterogeneous cellular networks," *IEEE J. Sel. Areas Commun.*, vol. 30, no. 3, pp. 550–560, Apr. 2012.

[29] S. Singh, H. S. Dhillon, and J. G. Andrews, "Offloading in heterogeneous networks: Modeling, analysis, and design insights," *IEEE Trans. Wireless Commun.*, vol. 12, no. 5, pp. 2484–2497, May 2013.

[30] M. D. Renzo, A. Guidotti, and G. E. Corazza, "Average rate of downlink heterogeneous cellular networks over generalized fading channels: A stochastic geometry approach," *IEEE Trans. Commun.*, vol. 61, no. 7, pp. 3050–3071, July 2013.

[31] H. ElSawy and E. Hossain, "On stochastic geometry modeling of cellular uplink transmission with truncated channel inversion power control," *IEEE Trans. Wireless Commun.*, vol. 13, no. 8, pp. 4454–4469, Aug. 2014.

[32] S. Singh, X. Zhang, and J. G. Andrews, "Joint rate and sinr coverage analysis for decoupled uplink-downlink biased cell associations in hetnets," *IEEE Trans. Wireless Commun.*, vol. 14, no. 10, pp. 5360–5373, Oct. 2015.

[33] T. Bai and R. W. Heath, "Coverage and rate analysis for millimeter-wave

cellular networks," *IEEE Trans. Wireless Commun.*, vol. 14, no. 2, pp. 1100–1114, Feb. 2015.
[34] S. Singh, M. N. Kulkarni, A. Ghosh, and J. G. Andrews, "Tractable model for rate in self-backhauled millimeter wave cellular networks," *IEEE J. Sel. Areas Commun.*, vol. 33, no. 10, pp. 2196–2211, Oct. 2015.
[35] M. D. Renzo, "Stochastic geometry modeling and analysis of multi-tier millimeter wave cellular networks," *IEEE Trans. Wireless Commun.*, vol. 14, no. 9, pp. 5038–5057, Sep. 2015.
[36] Z. Tong and M. Haenggi, "Throughput analysis for full-duplex wireless networks with imperfect self-interference cancellation," *IEEE Trans. Commun.*, vol. 63, no. 11, pp. 4490–4500, Nov. 2015.
[37] A. AlAmmouri, H. ElSawy, and M. S. Alouini, "Flexible design for α-duplex communications in multi-tier cellular networks," *IEEE Trans. Commun.*, vol. 64, no. 8, pp. 3548–3562, Aug. 2016.
[38] W. Lu and M. D. Renzo, "Stochastic geometry modeling and system-level analysis/optimization of relay-aided downlink cellular networks," *IEEE Trans. Commun.*, vol. 63, no. 11, pp. 4063–4085, Nov. 2015.
[39] J. N. Laneman, D. N. C. Tse, and G. W. Wornell, "Cooperative diversity in wireless networks: Efficient protocols and outage behavior," *IEEE Trans. Inf. Theory*, vol. 50, no. 12, pp. 3062–3080, Dec. 2004.
[40] K. Ntontin, M. D. Renzo, and C. Verikoukis, "System-level performance analysis of relay-aided multiple-antenna cellular networks," in *2016 IEEE 27th Annual International Symposium on Personal, Indoor, and Mobile Radio Communications (PIMRC)*, Sep. 2016.
[41] T. L. Marzetta, "Noncooperative cellular wireless with unlimited numbers of base station antennas," *IEEE Trans. Wireless Commun.*, vol. 9, no. 11, pp. 3590–3600, Nov. 2010.
[42] H. Cui, M. Ma, L. Song, and B. Jiao, "Relay selection for two-way full duplex relay networks with amplify-and-forward protocol," *IEEE Trans. Wireless Commun.*, vol. 13, no. 7, pp. 3768–3777, July 2014.
[43] J. Zhang, B. Zhang, S. Chen, X. Mu, M. El-Hajjar, and L. Hanzo, "Pilot contamination elimination for large-scale multiple-antenna aided ofdm systems," *IEEE J. Sel. Topics Signal Process.*, vol. 8, no. 5, pp. 759–772, Oct. 2014.
[44] F. Baccelli, *Stochastic geometry and wireless networks*. Hanover, Mass: Now Publishers, 2009.
[45] G. L. Stüber, *Principles of Mobile Communication*. Springer, 2013.
[46] B. Debaillie, D. J. van den Broek, C. Lavín, B. van Liempd, E. A. M. Klumperink, C. Palacios, J. Craninckx, B. Nauta, and A. Pärssinen, "Analog/rf solutions enabling compact full-duplex radios," *IEEE J. Sel. Areas Commun.*, vol. 32, no. 9, pp. 1662–1673, Sep. 2014.
[47] F. Jarai-Szabo and Z. Neda, "On the size-distribution of Poisson Voronoi cells," *eprint arXiv:cond-mat/0406116*, 2004.
[48] T. K. Y. Lo, "Maximum ratio transmission," *IEEE Trans. Commun.*, vol. 47, no. 10, pp. 1458–1461, Oct. 1999.
[49] K. Ntontin, M. D. Renzo, and C. Verikoukis, "On the feasibility of full-duplex relaying in multiple-antenna cellular networks," https://www.researchgate.net/publication/313422677.
[50] M. D. Renzo and W. Lu, "End-to-end error probability and diversity analysis of af-based dual-hop cooperative relaying in a poisson field of interferers at the destination," *IEEE Trans. Commun.*, vol. 14, no. 1, pp. 15–32, Jan. 2015.
[51] K. Davaslioglu and E. Ayanoglu, "Interference-based cell selection in heterogenous networks," in *Inf. Theory and Applications Workshop (ITA), 2013*, Feb. 2013, pp. 1–6.

Konstantinos Ntontin (S'12–M'14) was born in Athens, Greece, in 1983. He received the Diploma in Electrical and Computer Engineering in 2006, the M. Sc. Degree in Wireless Systems in 2009, and the Ph. D. degree in 2015 from the University of Patras, Greece, the Royal Institute of Technology (KTH), Sweden, and the Technical University of Catalonia (UPC), Spain, respectively. He is the recipient of the 2013 IEEE COMMUNICATIONS LETTERS Exemplary Reviewer Certificate.

His research interests are related to the Physical Layer of wireless telecommunications and particularly to topics such as performance analysis in fading channels, MIMO systems, array beamforming, and stochastic modeling of wireless channels.

Marco Di Renzo (S'05–AM'07-M'09-SM'14) received the Laurea degree (cum laude) and the Ph.D. degree in electrical engineering from the University of L'Aquila, Italy, in 2003 and 2007, respectively, and the D.Sc. degree (Habilitation à diriger des recherches) from the University of Paris-Sud, France, in 2013. Since 2010, he has been a CNRS Associate Professor (Chargé de Recherche Titulaire CNRS) with the Laboratory of Signals and Systems, Paris-Saclay University-CNRS, CentraleSupélec, University of Paris-Sud, Paris, France. His research interests include wireless communications, communication theory, and stochastic geometry. He currently serves as an Editor of the IEEE COMMUNICATIONS LETTERS and the IEEE TRANSACTIONS ON COMMUNICATIONS. He is a Distinguished Lecturer of the IEEE Vehicular Technology Society. He is a recipient of several research distinctions, which include the 2013 Network of Excellence NEWCOM# Best Paper Award, the 2013 IEEE-COMSOC Best Young Researcher Award for Europe, Middle East and Africa (EMEA Region), the 2015 IEEE Jack Neubauer Memorial Best System Paper Award, the 2015 Distinguished Visiting Fellow of the Royal Academy of Engineering, U.K., and the 2015-2018 CNRS Award for Excellence in Research and in Advising Doctoral Students.

Christos Verikoukis (S'95–M'04–SM'07) got his Ph.D. from UPC in 2000. He is currently a senior researcher at CTTC/CERCA and an adjunct professor at the University of Barcelona. He has published 100 journal papers and over 170 conference papers. He is also a co-author of three books, 14 chapters in other books, and two patents. He has participated in more than 30 competitive projects and has served as the principal investigator of national projects in Greece and Spain. He has supervised 15 Ph.D. students and five postdoctoral researchers since 2004. He was General Chair of the 17th, 18th and 19th IEEE CAMAD, the TPC Chair of the 6th IEEE Latincom and TPC Co-Chair of the 15th Healthcom. He has also served as the CQRM symposium co-chair in the IEEE Globecom 2014 & 2016 and IEEE ICC 2015 & 2016. He is currently Chair of the IEEE ComSoc CSIM TC. He received a best paper award in IEEE ICC 2011, IEEE Globecom 2014 & 2015, in EURACON/EUCNC 2016 as well as the EURASIP 2013 Best Paper Award for the Journal on Advances in Signal Processing.